



Analogs design, synthesis and biological evaluation of peptidomimetics with potential anti-HCV activity



Deena S. Lasheen^a, Mohamed A.H. Ismail^a, Dalal A. Abou El Ella^a, Nasser S.M. Ismail^a, Sameh Eid^b, Susan Vleck^c, Jeffrey S. Glenn^c, Andrew G. Watts^d, Khaled A.M. Abouzid^{a,*}

^a Pharmaceutical Chemistry Department, Faculty of Pharmacy, Ain Shams University, Cairo 11566, Egypt

^b Institute of Molecular Pharmacy, Pharmazentrum, University of Basel, Klingelbergstrasse 50, CH-4056 Basel, Switzerland

^c Division of Gastroenterology and Hepatology, Stanford University School of Medicine, Stanford, CA 94305-5187, USA

^d Department of Pharmacy and Pharmacology, University of Bath, Bath BA2 7AY, UK

ARTICLE INFO

Article history:

Received 16 December 2012

Revised 23 February 2013

Accepted 3 March 2013

Available online 24 March 2013

Keywords:

HCV NS3/4A protease inhibitors

Peptidomimetics

Vinyl sulfonates

Molecular modeling

Covalent docking

ABSTRACT

Two series of peptidomimetics were designed, prepared and evaluated for their anti-HCV activity. One series possesses a C-terminal carboxylate functionality. In the other series, the electrophilic vinyl sulfonate moiety was introduced as a novel class of HCV NS3/4A protease inhibitors. In vitro based studies were then performed to evaluate the efficacies of the inhibitors using Human hepatoma cells, with the vinyl sulfonate ester (**10**) in particular, found to have highly potent anti-HCV activity with an $EC_{50} = 0.296 \mu\text{M}$. Finally, molecular modeling studies were performed through docking of the synthesized compounds in the HCV NS3/4A protease active site to assess their binding modes with the enzyme and gain further insight into their structure–activity relationships.

© 2013 Elsevier Ltd. All rights reserved.

1. Introduction

In 2007, the WHO declared Hepatitis C virus (HCV) infection as a global health problem, with an estimate of more than 170 million infected people worldwide.¹ The disease has been described as a 'silent epidemic' and a 'serious health crisis'. About 80% of the infected cases develop chronic hepatitis, a condition that is incurable in many patients, and without therapeutic intervention, it can lead to morbidity or mortality within 10–20 years through either cirrhosis and hepatic failure or hepatocellular carcinoma.² Despite considerable reduction of the incidence of new infections, the prevalence of HCV infection is predicted to remain constant in the near future. Until recently, the standard of care (SOC) for HCV infection has been based on a combination therapy of injectable pegylated-interferon- α (peg-IFN- α) with oral ribavirin, which resulted in sustained virological response (SVR) rates of only 50% in patients with HCV-genotype 1 infection compared to almost 70–80% for genotypes 2 and 3.^{1–4} Furthermore, this former SOC had suffered from several drawbacks; being lengthy, expensive and accompanied by significant adverse effects.^{1,2,4} Other factors such as race, age, body weight, viral level and genotype also influenced the success of treatment.⁵ However, The introduction of first

generation protease inhibitors, boceprevir or telaprevir, to this SOC has dramatically changed the treatment of HCV-1 infected patients.^{6,7} Boceprevir or Telaprevir-based triple regimens have improved SVR rates by at least 25–30% compared to the former dual therapy. In addition, the duration of therapy can be reduced in more than half of the patients to 24–28 weeks compared to the conventional 48 weeks therapy.^{6–8}

HCV is a Flavivirus, with a single stranded, positive sense RNA genome of approximately 9600 nucleotides.⁹ This genome codes for a single polyprotein that is co- and post-translationally cleaved into 10 small proteins including structural (capsid, envelope glycoproteins) or (Core protein, E1 and E2), p7 and non-structural (NS2, NS3, NS4A, NS4B, NS5A, and NS5B) proteins.¹⁰ Most of the viral structural and non-structural proteins have been identified as potential anti-HCV targets; however, the NS3 protease with its NS4A cofactor remains one of the most promising targets due to its crucial role in the viral polyprotein processing and hence viral replication.¹¹ Moreover, clinical data derived from several protease inhibitors tested on HCV infected patients has clearly shown that protease inhibition is associated with a rapid decline in viral load.^{3,12} X-ray crystal structure of the full length NS3 protein has revealed a C-terminal helicase domain, and an N-terminal protease with a typical chymotrypsin-like fold, in addition to a structural a zinc binding site. It has also revealed the non-covalent association of the NS4A cofactor which is essential for the activation of the

* Corresponding author. Tel.: +20 1222165624; fax: +20 225080728.

E-mail address: Khaled.abouzid@pharm.asu.edu.eg (K.A.M. Abouzid).

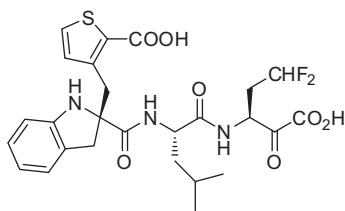


Figure 1. HCV protease inhibitor (**1**) $IC_{50} = 0.7 \mu M$.

protease. The protease active site has been shown to be situated at the interface between the helicase and the protease domains, creating a well-defined binding cleft.¹³ Several peptidic and peptidomimetic NS3/4A protease inhibitors that possess either a C-terminal acidic functionality or an electrophilic serine trap have been reported.^{14–21} Ontoria et al.²² have proposed a structure–activity relationship (SAR) and disclosed enzyme bound crystal structure for indoline based peptidomimetic inhibitor (**1**) (Fig. 1), however, further improvement of activity was still needed.

2. Rationale and design

In this investigation, a structure-guided strategy was used to design a series of peptidomimetic HCV NS3/4A protease inhibitors that either possess a C-terminal carboxylate functionality to mimic the product-based inhibitors, or an electrophilic vinyl sulfonate moiety which is proposed to act as a Michael acceptor to be attacked by the catalytic serine to form a covalent bond with the protease enzyme. The vinyl sulfonate group was chosen being a novel class of HCV protease inhibitors that have never been reported before as serine protease inhibitors but have proven successful as Michael acceptors capable of covalently inhibiting several cysteine and threonine proteases.^{23–27} Vinyl sulfonates have been reported to be capable of inactivating several cysteine proteases through irreversible addition of the thiol group of active site cysteine to the electrophilic vinyl sulfonate moiety. This addition reaction is catalyzed by histidine and aspartate residues present within the active site of the protease.²⁸

The design of these target molecules was based on modification of the indoline-based peptidomimetic inhibitor (**1**),²² by performing specific bioisosteric replacements in the indoline lead. The carboxylic head, or the vinyl sulfonate functionality, was proposed to occupy the oxyanion hole of the protease binding site. Several P1 amino acids were introduced replacing the difluoroethyl group of (**1**). Amino acids with non-bulky side chains were selected, to be accommodated within the rather small hydrophobic S1 pocket,¹³ such as alanine, valine, phenylalanine and threonine; which was

chosen to mimic the P1 amino acid at the natural NS3–NS4A substrate cleavage site so was proposed to be better recognized by the enzyme. The indoline ring was also replaced with a variety of arylidene moieties to study their interaction pattern with the protease binding site. A five-atom linker containing two hydrogen bond acceptors and one hydrogen bond donor was retained to maintain the hydrogen bonding interactions with the backbones of Ala157 and Arg155. An arylidene functionality was also introduced that could also serve as an additional Michael acceptor group that may be capable of interacting with the protease in a similar pattern.

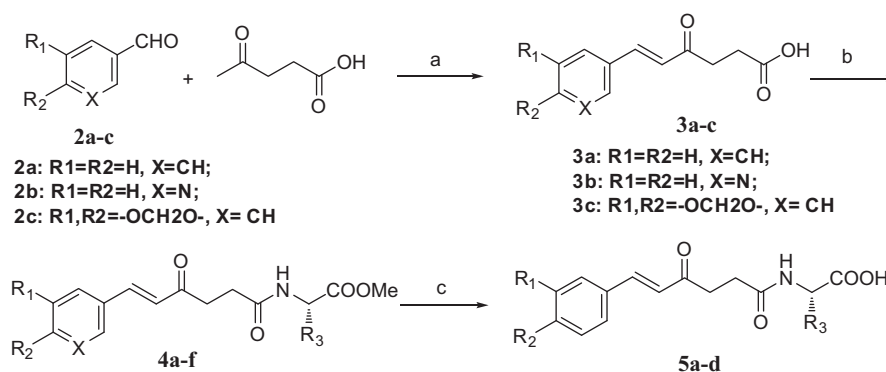
This design was further supported by molecular modeling studies, through docking of the designed molecules in the HCV NS3/4A protease binding site to assess their binding modes with the protease active site.

3. Results and discussion

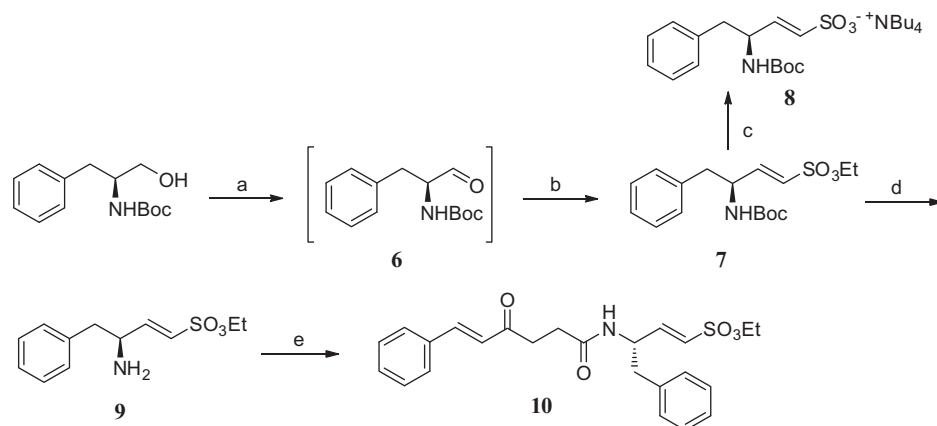
3.1. Chemistry

For the synthesis of the target esters (**4a–f**) and their corresponding acids (**5a–d**), the following straight forward pathway was pursued (Scheme 1). This involved the condensation of the corresponding aldehydes (**2a–c**) with levulinic acid using catalytic amounts of piperidine and acetic acid in refluxing benzene with the azeotropic removal of water using a Dean–Stark trap to afford the aryl oxohexenoic acids (**3a–c**) following reported methods.²⁹ ¹H NMR confirmed the formation of *E*-isomers with $J = 16$ Hz. Mixed anhydride approach using ethyl chloroformate and Et₃N was adopted for the condensation of **3a–c** with the appropriate amino esters (viz.; L-alanine methyl ester HCl and L-valine methyl ester HCl) to afford the ester derivatives (**4a–f**).³⁰ The obtained esters were hydrolyzed to the carboxylic acids (**5a–d**) under mild conditions using lithium hydroxide at room temperature.³¹

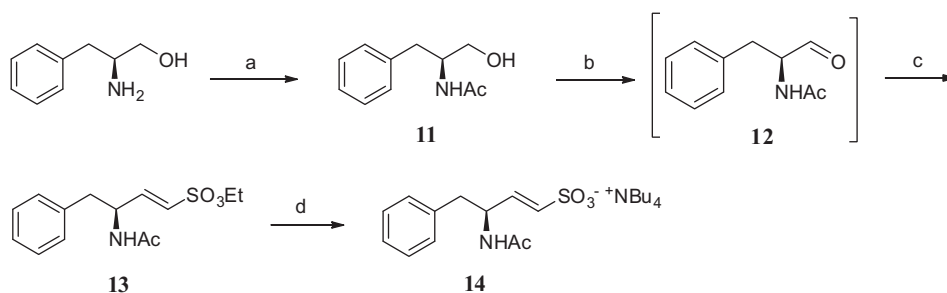
The introduction of vinyl sulfonate moiety was achieved via the sequence outlined in Scheme 2; Swern oxidation was employed for the conversion of Boc-L-phenylalaninol to its corresponding aldehyde (**6**) as previously reported.³² The Horner–Wadsworth–Emmons (HWE) olefination reaction with ethyl (diethoxyphosphoryl)-methanesulfonate³³ and *n*-Butyllithium (*n*-BuLi) at -78 °C gave the corresponding vinyl sulfonate (**7**) with complete (*E*) stereoselectivity.³⁴ Cleavage of the ethyl ester was effected by treatment of the sulfonate (**7**) with *n*-tetrabutylammonium iodide (*n*-Bu₄NI) in refluxing acetone following the reported procedure.³⁴ Boc deprotection of **7** was performed using 30% Trifluoroacetic acid (TFA) in CH₂Cl₂³⁵ to afford the rather unstable amine (**9**) which was used for the next step immediately after purification. Coupling of the amine (**9**) with the 6-phenyl-4-oxohex-5-enoic acid (**3a**) via a



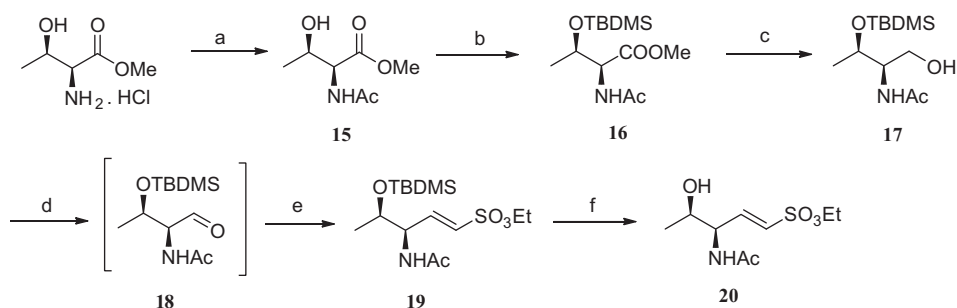
Scheme 1. Synthesis of 4-oxo-6-arylhex-5-enamidopropanoates and butanoates and their corresponding acids: Reagents and conditions: (a) Piperidine, AcOH, benzene, reflux, 14–16 h, 73–88%; (b) NH₂CH(R₃)COOMe, ethyl chloroformate, Et₃N, CH₂Cl₂, rt, 2 days, 46–50%; (c) LiOH·H₂O, THF/ethanol, rt, 2 h, 65–72%.



Scheme 2. Synthesis of L-phenylalanine-derived vinyl sulfonates and their corresponding salts: Reagents and conditions: (a) $(\text{COCl})_2$, DMSO, -63°C , 96%; (b) ethyl (diethoxyphosphoryl)methanesulfonate, *n*-BuLi, -78°C , 1 h, 72%; (c) Bu_4NI , acetone, reflux, 2 days, 94%; (d) TFA/ CH_2Cl_2 , rt, 1 h, 98%; (e) **3a**, ethyl chloroformate, Et_3N , CH_2Cl_2 , rt, 2 days, 44%.



Scheme 3a. Synthesis of acetylated L-phenylalanine-derived vinyl sulfonates. Reagents and conditions: (a) Ac_2O (1.1 equiv), pyridine, -20°C , 4 h, 78%; (b) PDC, CH_2Cl_2 , rt, 1 h, 58%; (c) ethyl (diethoxyphosphoryl)methanesulfonate, *n*-BuLi, THF, -78°C , 70%; (d) Bu_4NI , acetone, reflux, 2 days, 78%.

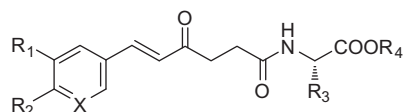


Scheme 3b. Synthesis of L-threonine-derived vinyl sulfonates: Reagents and conditions: (a) Et_3N , Ac_2O , pyridine, -20°C , 4 h, 88%; (b) TBDMS-Cl, imidazole, DMF, rt, 88%; (c) LiBH_4 , THF/MeOH, rt, 2 days, 84%; (d) $(\text{COCl})_2$, DMSO, CH_2Cl_2 , -63°C , 100%; (e) ethyl (diethoxyphosphoryl)methanesulfonate, *n*-BuLi, THF, -78°C , 59%; (f) 70% HF/pyridine, 3 h, rt, 86%.

mixed anhydride approach afforded the target L-phenylalanine-based vinyl sulfonate (**10**).

The acetylated L-phenylalanine- and L-threonine-based vinyl sulfonates were also prepared as probes to test the general ability of vinyl sulfonates to inhibit the HCV serine protease. Threonine was chosen to mimic the P1 amino acid in the natural NS3–NS4A substrate cleavage site so was proposed to be well recognized by the enzyme. The synthesis of these probes was pursued via the chemical pathways outlined in Schemes 3a and 3b; Thus for preparing the acetylated L-phenylalanine-based vinyl sulfonate (**13**), L-phenylalaninol was selectively N-acetylated using acetic anhydride in pyridine at -20°C , modifying a reported procedure.³⁶ It is worth noting that performing the acetylation at 0°C afforded the diacetyl derivative, but when the reaction was carried out at

a temperature not exceeding -20°C , the more nucleophilic amino group was selectively acetylated, with only traces of the diacetyl side product which was easily purified by silica chromatography. Oxidation using pyridinium dichromate (PDC)^{37,38} followed by HWE coupling afforded the vinyl sulfonate (**13**) which was subsequently converted to its tetrabutylammonium salt (**14**).³⁴ The L-threonine based vinyl sulfonate (**20**) was prepared via initial N-acetylation of L-threonine methyl ester HCl at -20°C as previously reported.³⁹ The threonine hydroxyl group was then protected as its *tert*-butyldimethylsilyl (TBDMS) ether following the reported procedure.⁴⁰ LiBH_4 in THF/MeOH (1:1)⁴¹ was employed for the reduction of the *O*-TBDMS-N-acetyl-L-threonine methyl ester (**16**) to provide the desired threoninol product (**17**) in 84% yield, which was then oxidized under Swern conditions to the corresponding

Table 1EC₅₀ and CC₅₀ for the carboxylate series of compounds assayed for their anti-HCV activity and cell viability, together with their safety indices (CC₅₀/EC₅₀)

Compd no	R ₁ R ₂	X	R ₃	R ₄	EC ₅₀ (μM)	CC ₅₀ (μM)	Safety index
Boceprevir	—	—	—	—	0.8	>100	—
4a	H	CH	CH ₃	CH ₃	0.960	1.318	1.373
4b	H	CH	CH(CH ₃) ₂	CH ₃	0.381	1.477	3.877
4c	H	N	CH ₃	CH ₃	0.900	2.108	2.342
4d	H	N	CH(CH ₃) ₂	CH ₃	1.141	1.571	1.377
4e	–OCH ₂ O–	CH	CH ₃	CH ₃	0.347	1.107	3.19
4f	–OCH ₂ O–	CH	CH(CH ₃) ₂	CH ₃	0.682	1.393	2.83
5b	H	CH	CH(CH ₃) ₂	H	22.476	>100	>4.45
5c	–OCH ₂ O–	CH	CH ₃	H	5.435	12.088	2.224

EC₅₀: half the maximal effective concentration, CC₅₀: 50% cytotoxicity concentration.**Table 2**EC₅₀ and CC₅₀ for vinyl sulfonate series of compounds assayed for their anti-HCV activity (genotype **2a**) and cell viability, together with their safety indices (CC₅₀/EC₅₀)

Compd no.	Structure	EC ₅₀ (μM)	CC ₅₀ (μM)	Safety index
7		1.213	3.500	2.885
8		8.621	67.029	7.775
10		0.296	~1	NA
13		2.110	7.907	3.747
14		8.690	>100	>11.5
20		4.360	27.706	6.355

aldehyde (**18**) in quantitative yield. HWE coupling of **18** with ethyl (diethoxyphosphoryl)-methanesulfonate followed by silyl deprotection using 70% HF in pyridine^{42,43} afforded the target L-threonine-based vinyl sulfonate (**20**).

3.2. Biological evaluation

The target compounds (**4a–f**, **5b**, **c**, **7**, **8**, **10**, **13**, **14**, **20**) were then evaluated for their ability to inhibit HCV replication in an in vitro cell culture system using Huh7.5 (Human hepatoma) cells which are highly permissive for the initiation of HCV replication.⁴⁴ The NS3 protease inhibitor, boceprevir (SCH503034)^{18,45} was used as a positive control. J6/JFH HCV RNA (genotype 2a) harboring a *Renilla* luciferase reporter gene was transfected into Huh7.5 cells by Liposome-mediated transfection using Lipofectamine 2000 (Invitrogen). Cells were grown in the presence of various nanomolar and micromolar concentrations of each of the test compounds for 48 h, after which the cells were subjected to luciferase assays and alamarBlue-based viability assays adopting reported procedures.^{46,47}

Luciferase assay performed revealed that all test compounds, except for **5b**, demonstrated potent inhibitory activity on HCV RNA replication, with EC₅₀s in submicromolar or low micromolar range (Tables 1 and 2). Most notably, the vinyl sulfonate **10**

(EC₅₀ = 0.296 μM), and the carboxylate esters **4b**, **4e** and **4f** (EC₅₀s = 0.381, 0.347 and 0.682, respectively) exhibited more potent HCV RNA inhibitory activity on genotype 2a than the positive control boceprevir (phase III clinical trials) (EC₅₀ = 0.8 μM). However, alamarBlue viability assays performed on individual compounds over the same concentration ranges demonstrated reduced cell viability associated with most of the test compounds, with the exception of compounds **5b** and **14**, which demonstrated no observable cellular toxicity within the studied range.

Thus, it has been observed that the carboxylate esters were much more potent than their corresponding acids (**4b**, **4e** vs **5b**, **5c**) however, acids were much less toxic. The vinyl sulfonate ester (**10**) exhibited the most potent anti-HCV activity, which was expected since it is more extended towards the S3 subsite of the enzyme. However, it demonstrated marked cellular toxicity. The phenylalanine derived vinyl sulfonate esters (**7** and **13**) were generally more potent (EC₅₀s = 1.213 and 2.110 μM, respectively) than their corresponding tetrabutylammonium salts (**8** and **14**) (EC₅₀s = 8.621 and 8.690 μM, respectively). However, salts seem to be less toxic. The threonine derived vinyl sulfonate ester (**20**) exhibited significant inhibitory activity on HCV replication (EC₅₀ = 4.36 μM) as well as an acceptable safety profile (CC₅₀ = 27.706), hence, may be considered a good candidate for further optimization, in order to increase the anti-HCV potency.

3.3. Molecular modeling

The prepared final compounds (**4a–f**, **5b**, **c**, **7**, **8**, **10**, **13**, **14**, **20**) were subjected to detailed docking studies performed to predict their binding modes to the HCV NS3/4A protease active site. These studies have successfully identified reasonable binding poses for all test molecules, with comparable docking scores, indicating that the proposed compounds could potentially bind to the HCV protease active site with comparable strengths. Two docking runs were done, an initial docking study, to assess the non-covalent binding interactions of all the studied molecules with the oxyanion hole and the other active site residues in the protease. This was followed by another docking study to test the ability of the vinyl sulfonate ester (**10**) to covalently bind to the catalytic Ser139.

3.3.1. Validation of docking methodology

Crystal structure of HCV protease in complex with the non-covalent macrocyclic inhibitor danoprevir (ITMN191) (PDB: 3M5L) was found to exhibit the highest resolution (1.25 Å) among other solved structures.⁴⁸ The co-crystallized ligand also showed reasonable resemblance to the inhibitors developed here, being peptidomimetic in nature, bearing an acidic head group, and a terminal aryl moiety; namely the fluoroisindoline substituent. This crystal structure was, thus, selected for non-covalent docking calculations. Another crucial reason for selecting this particular

crystal structure was that it has an Ile132 in place of Val132. In HCV-1a and 1b genotypes, position 132 is a valine residue, while in genotypes 2a and 2b it is replaced by Leu.⁴⁹ Given that biological assays were performed on HCV-2a, it was preferable to use a crystal structure where position 132 is occupied by an amino acid closer in size to Leu; namely Ile, as none of the available crystal structures contained a Leu132. However, a key residue in the S3 pocket of HCV protease, Cys159, is replaced by Ser159 in this crystal structure. Ontoria et al. designed indoline-based peptidomimetics bearing a thiophene ring to establish favorable contacts with the Cys159 residue in the lipophilic S3 pocket.²² On the other hand, Hagel et al. successfully designed irreversible covalently-bonded inhibitors targeting this non-catalytic cysteine, by means of attaching an acrylamide terminal group (a low-reactivity Michael acceptor) to a carefully designed scaffold.⁵⁰ For the purpose of this study, though, we decided to keep Ser159 unchanged since it is unlikely to have any detrimental effects on our docking studies.

The proposed docking algorithm was validated by self-docking of danoprevir, where it was removed from the complex (PDB: 3M5L) and then docked back into the binding site. Heavy-atom root mean square deviation (RMSD) values between top-ranked poses and the experimental crystal structure ranged from 0.4 to 1.4 Å (Fig. 2). Thus, Glide seemed to be an appropriate method for reliable prediction of docking poses for our compounds.

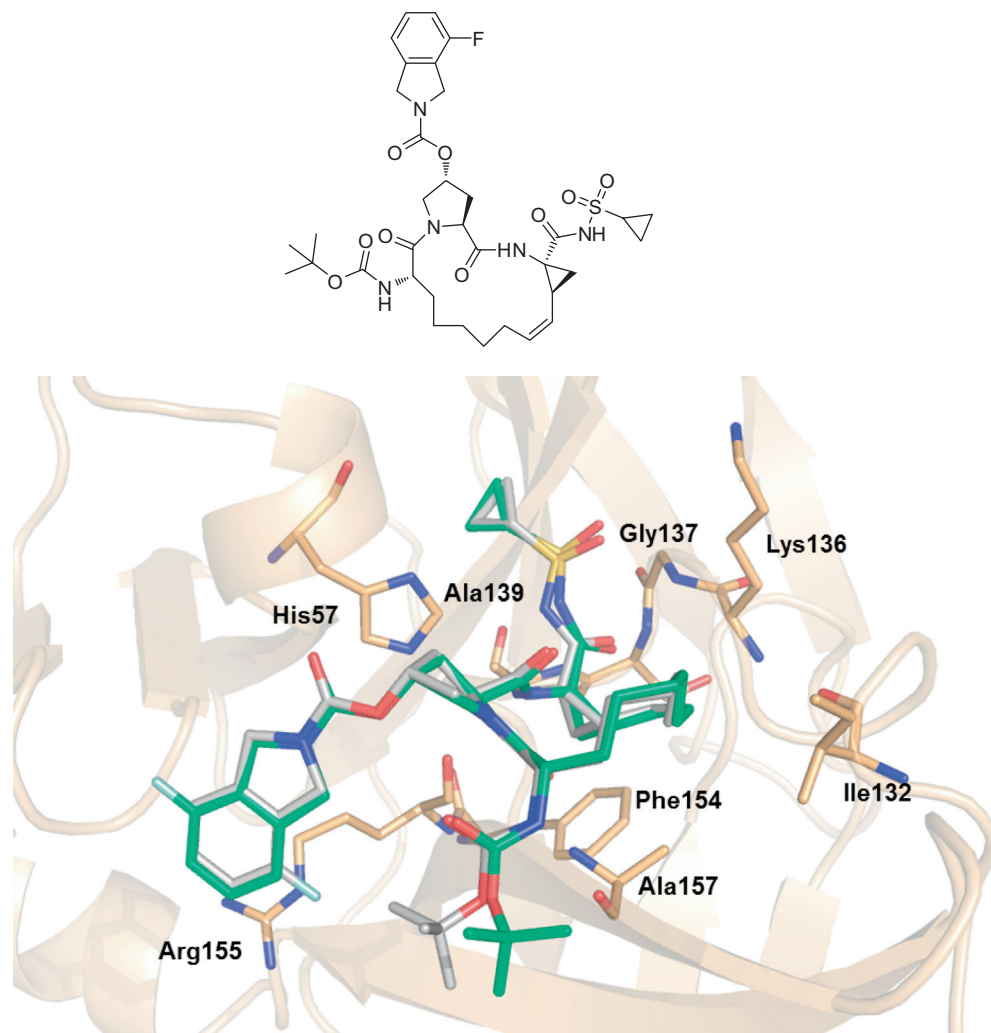


Figure 2. (Top) Structure of danoprevir (ITMN191), $IC_{50} < 0.25$ nM, $EC_{50} = 2.1$ nM. (Bottom) Results of self-docking of danoprevir (PDB code 3M5L); white carbons: crystal structure pose, green carbons: top-ranked docking pose. Atom color codes: N: blue, O: red, S: yellow, F: turquoise, hydrogen atoms are not shown.

It has been shown that binding site residues of HCV NS3/4A protease exhibit induced-fit conformational changes to adapt to various classes of ligands.^{51,48,52–54} Superposition of the active sites of boceprevir crystal structure (PDB: 2OC8) and the protease model employed in non-covalent docking (PDB: 3M5L) revealed a significant difference in side chain alignments (RMSD >3.7 Å). Docking of boceprevir to the rigid structure of 3M5L, which was employed in docking, would not be possible without allowing for readjustments of protein side chains. Therefore, docking of boceprevir to 3M5L has been a good challenge to test the induced-fit docking procedure. Induced-fit docking of boceprevir to 3M5L structure successfully retrieved poses having RMSD values of ~1.5 Å from the original crystal structure geometry (Fig. 3). This result confirmed the validity of the proposed induced-fit methodology in cases where some degree of receptor adaptation was to be expected, that is, with larger and/or more flexible ligands.

3.3.2. Glide docking

Top-ranked poses for all studied compounds were found to occupy the oxyanion hole and exhibited favorable hydrogen bonding and/or electrostatic interactions with backbone NH's of Gly137 and Ala139. In most cases, the acidic head groups (carboxylate or sulfonate) occupied the oxyanion hole, which confirmed our design

hypothesis. For some compounds however, different binding modes were also observed where either the amide oxygen or enone oxygen of the inhibitor filled the oxyanion hole. These differences could be exemplified by comparing docking results for **4e** and **4f** (Fig. 4). The alanine-based (**4e**) occupied the oxyanion hole via its amide oxygen while in its valine-based analogue (**4f**) it was filled by the enone oxygen. Additionally, both compounds were predicted to extend deeper into the S3 pocket via their benzodioxole tail interacting favorably with Ser159, which could in part explain their superior anti-HCV activities demonstrated in vitro. Docking results of long flexible molecules, for example, **4c**, **4e**, and **10**, showed favorable interactions via their aromatic tail groups with Ser159 in S3 pocket. Hagel et al. recently exploited a similar scaffold to place a Michael acceptor in the vicinity of the analogous non-catalytic Cys159 in S3 pocket of HCV NS3/4A protease.⁵⁰ In our case, though, results from molecular docking did not retrieve any poses where the Michael acceptor group was close enough to the corresponding Ser159. This was not surprising, however, since the reactive groups in our molecules were fairly close to the oxyanion hole binding motif. Placing the reactive groups close to S3 pocket would, thus, result in breaking off all key interactions in the oxyanion hole, and consequently the molecules would not be able to bind to the active site.

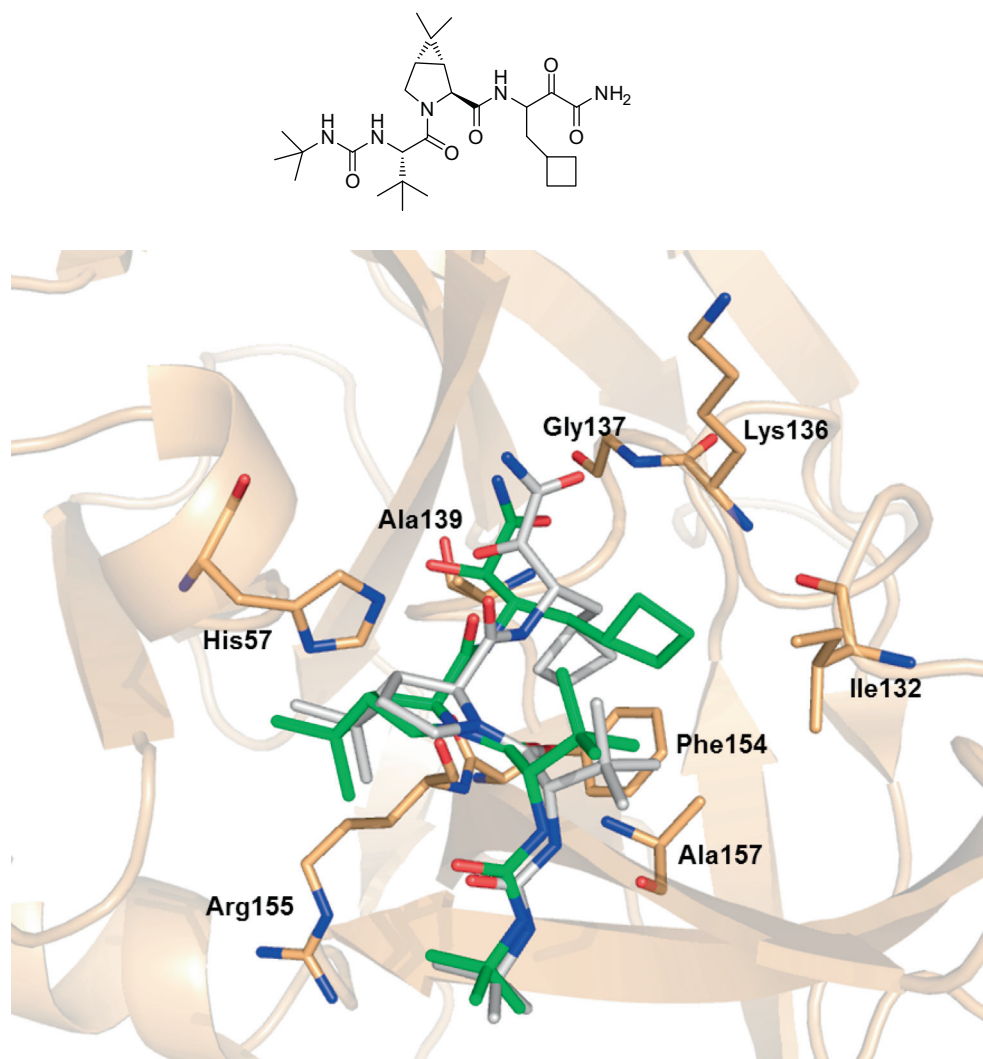


Figure 3. (Top) Structure of boceprevir. (Bottom) Results of induced-fit docking of boceprevir; white carbons: crystal structure pose from PDB 2OC8, green carbons: top-ranked docking pose to the receptor grid generated from PDB 3M5L. Atom color codes analogous to Figure 2.

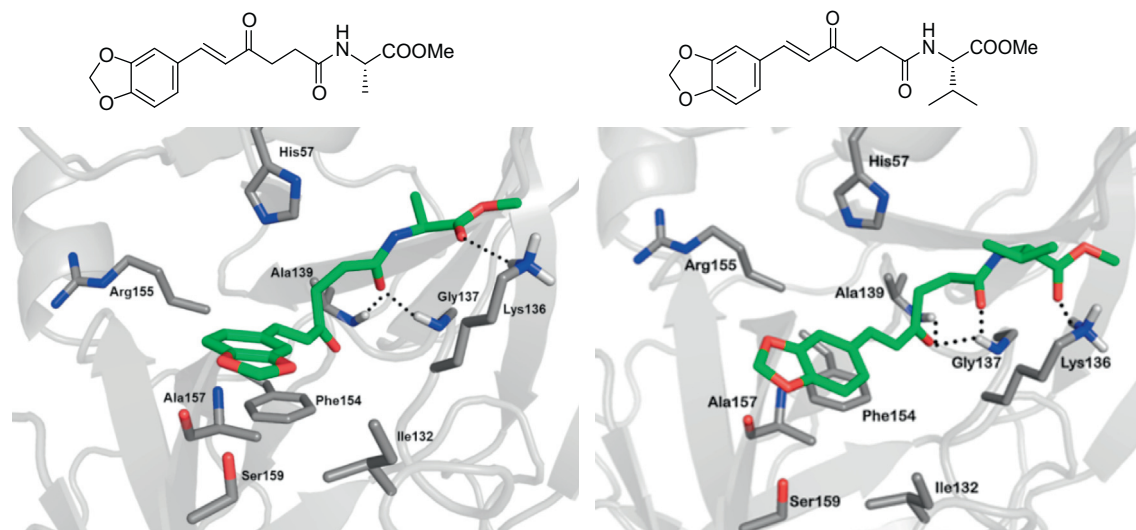


Figure 4. Top-ranked docking poses for compounds **4e** (left) and **4f** (right). The bulky benzodioxole interacts favourably with Ile132, Ala157 and extends even deeper in the S3 pocket reaching Ser159. Both compounds can also form H-bonds with the side chain of Lys136 via their carboxylate moieties.

Table 3

Docking scores and interaction fingerprints for the docking poses of modelled compounds; residues defining interaction subsites are given below the table

Compd no.	Glide score (kcal/mol)	Oxyanion hole	S1	S2	S3
4a	−3.00	−7.15	−5.62	−6.20	−14.56
4b	−4.95	−2.88	−8.62	−13.48	−9.43
4c	−3.42	−7.72	−6.46	−4.79	−20.77
4d	−4.91	−2.64	−8.53	−13.05	−9.22
4e	−4.65	−7.83	−5.95	−7.67	−16.04
4f	−5.03	−6.21	−4.59	−13.74	−4.44
5b	−4.99	−10.25	−3.97	−13.31	−66.04
5c	−4.72	−15.08	−0.58	−22.76	−34.35
7	−4.61	−8.48	−6.20	−11.94	−10.78
8	−4.72	−8.71	−2.41	−12.55	−58.93
10	−5.91 ^a	−4.40 ^a	−6.37 ^a	−16.99 ^a	−8.65 ^a
13	−3.70	−4.73	−3.72	−8.25	−11.21
14	−4.38	−9.75	0.17	−11.43	−56.96
20	−5.11	−10.23	−0.40	−3.72	−9.29

Oxyanion hole: Σ (Gly137, Ala139).

S1: Σ (Ala157, Ile132, Phe154).

S2: Σ (Ala157, Arg155, His57).

S3: Σ (Ile132, Ala157, Ser159, Lys136, Arg161).

^a Score of the pose obtained from induced-fit docking.

Table 3 lists the interaction fingerprints for the studied compounds (see Section 5.2.1 for details on calculation, and Figs. S2 and S3 in Supplementary data for plots). Analysis of the interaction fingerprints for the carboxylate series revealed different subsite preferences for the different structural classes. Although interactions of the carboxylate derivatives with the oxyanion hole were of comparable strengths; they differed with respect to interaction with S2 and S3 subsites. The alanine-based derivatives (**4a**, **4c**, and **4e**) tended to occupy the oxyanion hole via their amide oxygen, which allowed the carboxymethyl group to make a hydrogen bond with Lys136 in S3 pocket, or even a stronger salt bridge in case of compound **5c**. On the other hand, the oxyanion hole was occupied via carboxylate or enone oxygen in case of valine-based carboxylate derivatives (**4b**, **4d** and **4f**). Molecular orientation was, thus, different from the alanine-based series since the molecules' tails generally packed against Arg155 side chain and other carbonyl groups made H-bonds to Ala157 in S2 pocket (Comparison between **4a** and **4b** is given in Fig. S1 in Supplementary

data). The relative strengths of S2/S3 interaction energies were, thus, reversed in favor of S2 in valine-based compounds in contrast to their alanine-based counterparts (Fig. S2 in Supplementary data).

3.3.3. Induced-fit docking

Due to its larger size, compound (**10**) was also subjected to the more time consuming induced-fit docking procedure. This compound displayed the most extensive network of interactions in the HCV protease binding site (Fig. 5). In agreement with the design rationale, the oxyanion hole was occupied by the sulfonate head group, which made two strong hydrogen bonds to backbone NHs of Gly137 and Ala139. The phenylalanine moiety was situated between S1 and S3 pockets interacting with side chains of Ile132, Phe154 and Ala157. The central part of the ligand wrapped around His57 in S2 while the central amide NH was H-bonded to backbone carbonyl of Arg155. The arylidene tail packed against the side chain of Arg155 in the S2 subsite.

3.3.4. Prime covalent docking

As shown in Figure 5, the reactive vinyl group of (**10**) is situated appropriately in the catalytic site. The distance between the β -carbon of Ala139 and the electropositive vinyl carbon was as low as 4.5 Å, which could facilitate Michael-type nucleophilic attack on the labile carbon. Prime covalent docking of (**10**) study revealed that upon covalent binding, the ligand could be well accommodated within HCV protease active site. Most of the interactions observed in the non-covalent docking were conserved upon covalent addition of Ser139, although some active site residues had to undergo significant re-arrangement, especially His57, Lys136 and Arg155. The top-ranked poses showed that after covalent binding, compound (**10**) could either fill S1 and S3 pockets or S2 and S3 pockets (Fig. 6).

4. Conclusion

In conclusion, vinyl sulfonates were introduced as a novel class of peptidomimetic HCV NS3/4A protease inhibitors that has never been reported before as serine protease inhibitors. The vinyl sulfonate ester (**10**) exhibited highly potent anti-HCV activity in cell culture based assay ($EC_{50} = 0.296 \mu\text{M}$). This was further justified by docking studies, which revealed its capability of forming an

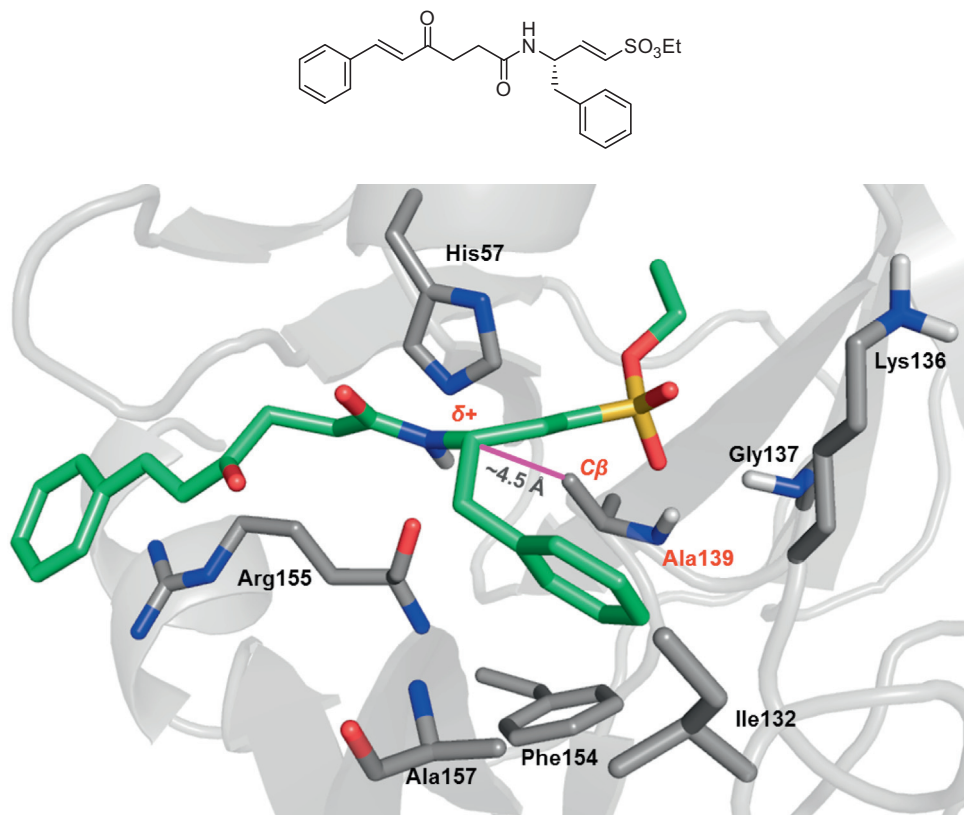


Figure 5. Induced-fit docking pose for compound (**10**). The distance between the beta carbon of Ala139 and the electropositive carbon susceptible to Michael-type attack is marked. Re-adjustments in active site residues allowed better interactions with HCV protease S1 (Ala157 and Phe154), S2 (Arg155 and His57), and S3 (Ile132 and Lys136) subsites.

extensive network of interactions with the oxyanion hole, and other non-prime pockets in the HCV protease binding site. Also, the predicted poses placed the electropositive vinyl carbon in close vicinity to the catalytic OH of Ser139, which could facilitate a Michael-type addition reaction. In addition, another series of peptidomimetic carboxylate-based HCV NS3/4A protease inhibitors have also been introduced. All the prepared carboxylate esters demonstrated potent anti-HCV inhibitory activity, with compounds (**4b** and **4e**) being the most potent ($EC_{50}S = 0.381$ and $0.347 \mu M$, respectively). The above apparent antiviral potencies, however, must be interpreted in light of corresponding relatively low $CC_{50}S$, which could account for a significant component of the $EC_{50}S$. Several compounds, however, exhibited considerably more favorable therapeutic indices (e.g., compounds **8** and **14**).

5. Experimental

5.1. Chemistry

5.1.1. Materials and instrumentation

Starting materials and reagents were purchased from Sigma–Aldrich or Acros Organics and used without further purification. Anhydrous methylene chloride was dried by distillation over calcium hydride. Anhydrous THF was dried by distillation over sodium/benzophenone. Anhydrous benzene was dried by distillation over Na metal. Other solvents are purchased from Fisher scientific or Sigma–Aldrich and used without further purification. Analytical thin layer chromatography (TLC) was performed on silica gel 60 F₂₅₄ packed on Aluminium sheets, purchased from Merck. Column chromatography was performed on silica 60 (35–70 microns) purchased from Fisher. Melting points were recorded

on Stuart Scientific apparatus and were uncorrected. 1H NMR spectra were recorded in δ scale given in ppm on a Joel 270 MHz spectrophotometer, or a Varian 400 MHz spectrophotometer, or a Varian 300 MHz and referred to TMS. ^{13}C NMR spectra were recorded on Varian spectrophotometer operating at 100 MHz. High resolution mass spectroscopy (HRMS) was performed on a Bruker MicroOTOF™ instrument coupled with an electrospray source (ESI-TOF). FT-IR spectra were recorded on a Perkin–Elmer spectrophotometer. Elemental analyses were performed at the Microanalytical Center, Cairo University.

5.1.2. (E)-4-Oxo-6-(pyridin-3-yl)hex-5-enoic acid (**3b**)

To a solution of pyridine-3-carbaldehyde (nicotinaldehyde) (20 mmol), and levulinic acid (2.32 g, 20 mmol) in dry benzene (60 mL), piperidine (0.25 mL, 2.5 mmol) and glacial acetic acid (0.8 mL, 14 mmol) were added. The solution was refluxed using a Dean–Stark apparatus until the disappearance of starting material as judged by TLC (14 h). The reaction was allowed to cool to rt, then the solvent was evaporated in vacuo. The residue was dissolved in EtOAc (50 mL), washed with 20% AcOH (2 × 20 mL), brine (2 × 20 mL), dried over anhydrous $MgSO_4$, and filtered. The filtrate was evaporated in vacuo then recrystallized from hot ethanol to afford the titled product (**3b**), as yellow crystals, (3 g, 73%); mp 176–178 °C; 1H NMR (300 MHz, $CDCl_3$): δ 8.76 (s, 1H, pyridyl), δ 8.63–8.62 (d, 1H, pyridyl), δ 7.88–7.85 (d, 1H, pyridyl), δ 7.62–7.58 (d, $J = 16$ Hz, 1H, py-CH=CH), δ 7.35–7.31 (m, 2H, pyridyl), δ 6.85–6.81 (d, $J = 16$ Hz, 1H, py-CH=CH), δ 3.06–2.99 (m, 2H, CO-CH₂-CH₂-COOH), δ 2.60–2.54 (m, 2H, CO-CH₂-CH₂-COOH); FT-IR (ν_{max} , cm^{-1}): 3400–2900 (OH carboxylic), 1715, 1694 (2 C=O), MS (Molecular formula: $C_{11}H_{11}NO_3$, Mwt.: 205.07): m/z 205.05 (M^+ , 31.11%), 103.65 (78.08%).

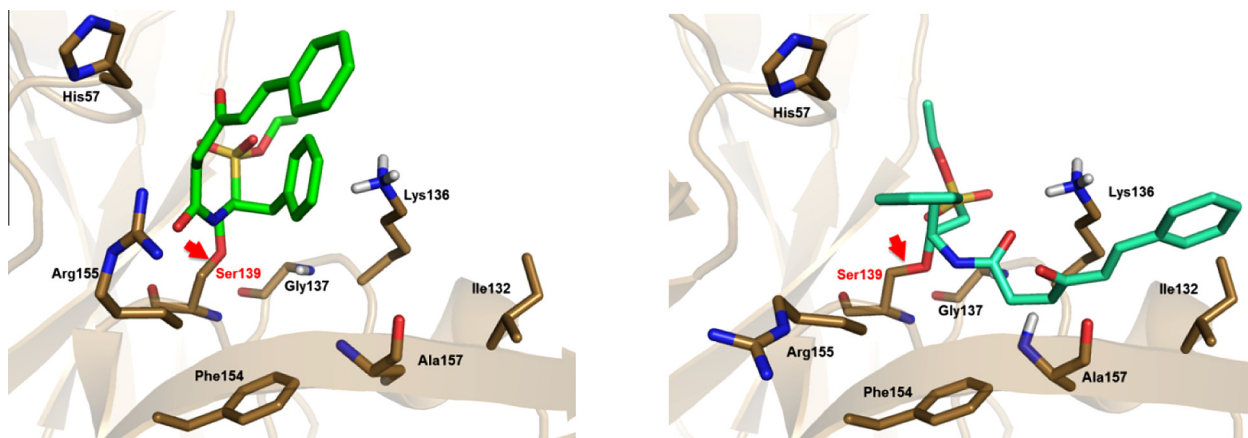


Figure 6. Covalent docking poses for compound (**10**): first top-ranked pose (left), second top-ranked pose (right). Covalent bond with catalytic Ser139 is marked with red arrow.

5.1.3. (*S,E*)-Methyl 2-(4-oxo-6-arylhex-5-enamido)propanoates and (*S,E*)-Methyl 3-methyl-2-(4-oxo-6-arylhex-5-enamido)butanoates (**4a–f**)

5.1.3.1. General procedure.

To an ice-cooled solution of the acid (**3a–c**) (3 mmol) and triethylamine (0.708 g, 7 mmol) in methylene chloride (10 mL) stirred at -10°C in an ice-salt bath, ethyl chloroformate (0.29 mL, 3 mmol) was added dropwise, and stirring was continued for 10 min, after which a solution of the respective amino acid ester hydrochloride salt (viz.; *L*-alanine methyl ester HCl or *L*-valine methyl ester HCl) in CH_2Cl_2 (3 mL) was added dropwise. The cooling bath was then removed and the reaction was stirred at rt for 2 days until the disappearance of the starting materials as judged by TLC. The solvent was evaporated in vacuo; the residue was dissolved in EtOAc (20 mL). The organic layer was washed with 10% HCl (2 \times 15 mL) then saturated Na_2CO_3 solution (2 \times 15 mL), dried over anhydrous MgSO_4 and filtered. The filtrate was evaporated in vacuo to afford the crude products (**4a–f**) which were purified by column chromatography.

5.1.3.2 (*S,E*)-Methyl 2-(4-oxo-6-phenylhex-5-enamido)propanoate (**4a**).

The titled compound was purified by column chromatography (gradient elution starting from 1% EtOAc/ CH_2Cl_2 and increasing polarity to 10% EtOAc/ CH_2Cl_2) to afford **4a** as buff crystals (0.4 g, 46%); mp $74\text{--}75^{\circ}\text{C}$; $^1\text{H NMR}$ (300 MHz, CDCl_3): δ 7.64–7.60 (d, $J = 16$ Hz, 1H, Ph-CH=CH), δ 7.59–7.54 (m, 3H, Ar), δ 7.42–7.39 (m, 2H, Ar), δ 6.79–6.74 (d, $J = 16$ Hz, 1H, Ph-CH=CH), δ 6.25 (br s, 1H, NH), δ 4.62–4.55 (q, 1H, NH-CH-CO₂Me), δ 3.76 (s, 3H, CO₂-CH₃), δ 3.11–3.00 (t, 2H, CO-CH₂-CH₂-CO), δ 2.64–2.55 (t, 2H, CO-CH₂-CH₂-CO), δ 1.44–1.39 (d, 3H, NHCH-CH₃); FT-IR (ν_{max} , cm^{-1}): 3315 (NH), 3055 (CH=CH), 1739 (C=O ester), 1689 (C=O ketone), 1672 (C=O amide); MS (Mwt.: 289.33): m/z 289.75 (M^+ , 28.18%), 187.20 (100%). Anal. Calcd for $\text{C}_{16}\text{H}_{19}\text{NO}_4$: C, 66.42; H, 6.62; N, 4.84. Found: C, 66.75; H, 6.42; N, 4.82.

5.1.3.3. (*S,E*)-Methyl 3-methyl-2-(4-oxo-6-phenylhex-5-enamido)butanoate (**4b**).

The titled compound was purified by column chromatography (gradient elution starting from 1% EtOAc/ CH_2Cl_2 and increasing polarity to 10% EtOAc/ CH_2Cl_2) to afford **4b** as buff crystals (0.48 g, 50%); mp $84\text{--}85^{\circ}\text{C}$; $^1\text{H NMR}$ (300 MHz, CDCl_3): δ 7.64–7.58 (d, $J = 16$ Hz, 1H, Ph-CH=CH), δ 7.57–7.54 (m, 3H, Ar), δ 7.42–7.39 (m, 2H, Ar), δ 6.79–6.74 (d, $J = 16$ Hz, 1H, Ph-CH=CH), δ 6.22–6.20 (br s, 1H, NH), δ 4.58–4.54 (m, 1H, NH-CH-CO₂Me), δ 3.75 (s, 3H, CO₂-CH₃), δ 3.13–3.04 (m, 2H, CO-CH₂-CH₂-CO), δ 2.67–2.61 (m, 2H, CO-CH₂-CH₂-CO), δ 2.18–2.16 (m, 1H, NHCH-CH), δ 0.97–0.92 (m, 6H, CH-(CH₃)₂); FT-IR (ν_{max} , cm^{-1}):

3318 (NH), 3069 (CH=CH), 2932, 2912 (CH aliphatic), 1735 (C=O ester), 1692 (C=O ketone), 1665 (C=O amide); MS (Mwt.: 317.38): m/z 317.60 (M^+ , 37.19%), 187.50 (100%). Anal. Calcd for $\text{C}_{18}\text{H}_{23}\text{NO}_4$: C, 68.12; H, 7.30; N, 4.41. Found: C, 68.36; H, 7.44; N, 4.51.

5.1.3.4 (*S,E*)-Methyl 2-(4-oxo-6-(pyridin-3-yl)hex-5-enamido)propanoate (**4c**).

This compound was purified by column chromatography (gradient elution starting from EtOAc then 1% MeOH/EtOAc and increasing polarity to 5% MeOH/EtOAc) to afford **4c** as pale yellow crystals (0.42 g, 48%); mp 116°C ; $^1\text{H NMR}$ (300 MHz, CDCl_3): δ 8.77 (s, 1H, pyridyl), δ 8.64–8.62 (d, 1H, pyridyl), δ 7.89–7.85 (d, 1H, pyridyl), δ 7.62–7.57 (d, $J = 16$ Hz, 1H, py-CH=CH), δ 7.34–7.32 (m, 1H, pyridyl), δ 6.86–6.80 (d, $J = 16$ Hz, 1H, py-CH=CH), δ 6.24 (br s, 1H, NH), δ 4.62–4.57 (m, 1H, NH-CH-CO₂Me), δ 3.76 (s, 3H, CO₂-CH₃), δ 3.15–3.00 (t, 2H, CO-CH₂-CH₂-CO), δ 2.65–2.58 (t, 2H, CO-CH₂-CH₂-CO), δ 1.44–1.36 (d, 3H, NHCH-CH₃); FT-IR (ν_{max} , cm^{-1}): 3321 (NH), 3056 (CH=CH), 1733 (C=O ester), 1694 (C=O ketone), 1670 (C=O amide); MS (Mwt.: 290.31): m/z 290.35 (M^+ , 1.05%), 188.00 (42.05%), 131.95 (100%). Anal. Calcd for $\text{C}_{15}\text{H}_{18}\text{N}_2\text{O}_4$: C, 62.06; H, 6.25; N, 9.65. Found: C, 62.09; H, 5.95; N, 9.72.

5.1.3.5 (*S,E*)-Methyl 3-methyl-2-(4-oxo-6-(pyridin-3-yl)hex-5-enamido)butanoate (**4d**).

The titled compound was purified by column chromatography (gradient elution starting from EtOAc then 1% MeOH/EtOAc and increasing polarity to 5% MeOH/EtOAc) to afford **4d** as pale yellow crystals (0.45 g, 47%); mp $76\text{--}77^{\circ}\text{C}$; $^1\text{H NMR}$ (300 MHz, CDCl_3): δ 8.76 (s, 1H, pyridyl), δ 8.62–8.61 (d, 1H, pyridyl), δ 7.88–7.84 (d, 1H, pyridyl), δ 7.62–7.56 (d, $J = 16$ Hz, 1H, py-CH=CH), δ 7.36–7.33 (m, 1H, pyridyl), δ 6.85–6.80 (d, $J = 16$ Hz, 1H, py-CH=CH), δ 6.21 (br s, 1H, NH), δ 4.58–4.53 (m, 1H, NH-CH-CO₂Me), δ 3.74 (s, 3H, CO₂-CH₃), δ 3.12–3.03 (m, 2H, CO-CH₂-CH₂-CO), δ 2.68–2.62 (m, 2H, CO-CH₂-CH₂-CO), δ 2.18–2.15 (m, 1H, NHCH-CH), δ 0.97–0.92 (m, 6H, CH-(CH₃)₂); FT-IR (ν_{max} , cm^{-1}): 3325 (NH), 3059 (CH=CH), 2966, 2910 (CH aliphatic), 1740 (C=O ester), 1684 (C=O ketone), 1665 (C=O amide); MS (Mwt.: 318.37): m/z 319.00 (M^+ , 34.19%), 259.15 (49.26%), 132.15 (100%). Anal. Calcd for $\text{C}_{17}\text{H}_{22}\text{N}_2\text{O}_4$: C, 64.13; H, 6.97; N, 8.80. Found: C, 64.21; H, 6.72; N, 8.86.

5.1.3.6 (*S,E*)-Methyl 2-(6-(benzo[d][1,3]dioxol-5-yl)-4-oxohex-5-enamido)propanoate (**4e**).

This titled compound was purified by column chromatography (gradient elution starting from 1% EtOAc/ CH_2Cl_2 and increasing

polarity to 20% EtOAc/CH₂Cl₂) to afford **4e** as orange buff crystals (0.48 g, 48%); mp 121–122 °C; ¹H NMR (300 MHz, CDCl₃): δ 7.55–7.49 (d, *J* = 16 Hz, 1H, Ph-CH=CH), δ 7.06 (s, 1H, Ph), δ 7.05–7.02 (d, *J* = 8 Hz, 1H, Ph), δ 6.84–6.82 (d, *J* = 8 Hz, 1H, Ph), δ 6.63–6.57 (d, *J* = 16 Hz, 1H, Ph-CH=CH), δ 6.26 (br s, 1H, NH), δ 6.00 (s, 2H, OCH₂O), δ 4.62–4.57 (m, 1H, NH-CH-CO₂Me), δ 3.76 (s, 3H, CO₂-CH₃), δ 3.07–3.00 (t, 2H, CO-CH₂-CH₂-CO), δ 2.62–2.58 (t, 2H, CO-CH₂-CH₂-CO), δ 1.43–1.40 (d, 3H, NHCH-CH₃); FT-IR (*v*'_{max}, cm⁻¹): 3310 (NH), 3052 (CH=CH), 2966 (CH aliphatic), 1729 (C=O ester), 1689 (C=O ketone), 1652 (C=O amide); MS (Mwt.: 333.34): *m/z* 333.55 (M⁺, 49.61%), 231.25 (100%). Anal. Calcd for C₁₇H₁₉NO₆: C, 61.25; H, 5.75; N, 4.20. Found: C, 61.47; H, 5.43; N, 4.51.

5.1.3.7 (S,E)-Methyl 2-(6-(benzo[d][1,3]dioxol-5-yl)-4-oxohex-5-enamido)-3-methyl-butanoate (**4f**).

The titled compound was purified by column chromatography (gradient elution starting from 1% EtOAc/CH₂Cl₂ and increasing polarity to 20% EtOAc/CH₂Cl₂) to afford **4f** as buff crystals (0.48 g, 48%); mp 77–78 °C; ¹H NMR (300 MHz, CDCl₃): δ 7.55–7.49 (d, *J* = 16 Hz, 1H, Ph-CH=CH), δ 7.05 (s, 1H, Ph), δ 7.05–7.02 (d, *J* = 8 Hz, 1H, Ph), δ 6.84–6.81 (d, *J* = 8 Hz, 1H, Ph), δ 6.63–6.57 (d, *J* = 16 Hz, 1H, Ph-CH=CH), δ 6.26–6.23 (br s, 1H, NH), δ 6.02 (s, 2H, OCH₂O), δ 4.57–4.53 (m, 1H, NH-CH-CO₂Me), δ 3.74–3.73 (s, 3H, CO₂-CH₃), δ 3.09–3.00 (m, 2H, CO-CH₂-CH₂-CO), δ 2.64–2.62 (m, 2H, CO-CH₂-CH₂-CO), 2.18–2.15 (q, 1H, NHCH-CH), δ 0.96–0.92 (m, 6H, CH-(CH₃)₂); FT-IR (*v*'_{max}, cm⁻¹): 3305 (NH), 3058 (CH=CH), 2957, 2910 (CH aliphatic), 1727 (C=O ester), 1690 (C=O ketone), 1615 (C=O amide); MS (Mwt.: 361.39): *m/z* 361.65 (M⁺, 53.72%), 174.70 (90.12%), 87.60 (100%). Anal. Calcd for C₁₉H₂₃NO₆: C, 63.15; H, 6.41; N, 3.88. Found: C, 63.06; H, 6.67; N, 3.70.

5.1.4. (S,E)-2-(4-Oxo-6-arylhex-5-enamido)propanoic acids and (S,E)-3-Methyl-2-(4-oxo-6-arylhex-5-enamido)butanoic acids (**5a–d**)

5.1.4.1. General procedure. To a stirred solution of the respective ester (**4a,b,e** and **f**) (0.7 mmol) in a 2:1 mixture of THF/ethanol (15 mL) at rt, aqueous solution of LiOH (70 mg, 3.5 mmol, in 6 mL H₂O) was added portionwise and the resulting solution was stirred at rt for 2–3 h until TLC (2% MeOH/EtOAc) revealed the disappearance of starting material. The solvent was partially removed in vacuo; EtOAc (20 mL) was then added followed by 1 N HCl solution (10 mL). The layers were separated, the aqueous phase was extracted with EtOAc (3 × 15 mL), the combined organic phase was dried over anhydrous MgSO₄ and filtered. The filtrate was evaporated in vacuo to afford the crude acid (**5a–d**) which was further purified by column chromatography (using gradient elution starting from EtOAc then 1% MeOH/EtOAc and increasing polarity to 5% MeOH/EtOAc).

5.1.4.2 (S,E)-2-(4-Oxo-6-phenylhex-5-enamido)propanoic acid (**5a**).

The titled acid was separated as yellow oil, (125 mg, 65%); ¹H NMR (300 MHz, CDCl₃): δ 7.64–7.59 (d, *J* = 16 Hz, 1H, Ph-CH=CH), δ 7.57–7.54 (m, 3H, Ar), δ 7.41–7.39 (m, 2H, Ar), δ 6.79–6.73 (d, *J* = 16 Hz, 1H, Ph-CH=CH), δ 6.54–6.52 (d, 1H, NH), δ 4.59–4.51 (m, 1H, NH-CH-CO₂H), δ 3.11–3.06 (t, 2H, CO-CH₂-CH₂-CO), δ 2.65–2.63 (t, 2H, CO-CH₂-CH₂-CO), δ 1.47–1.45 (d, 3H, NHCH-CH₃); FT-IR (*v*'_{max}, cm⁻¹): 3400–2900 (OH carboxylic), 1710, 1701 (2 C=O) 1665 (C=O amide); MS (Mwt.: 275.30): *m/z* 275.40 (M⁺, 1.12%), 131 (24.46%), 102.45 (50.96), 54.05 (100%). Anal. Calcd for C₁₅H₁₇NO₄: C, 65.44; H, 6.22; N, 5.09. Found: C, 65.32; H, 6.11; N, 5.22.

5.1.4.3 (S,E)-3-Methyl-2-(4-oxo-6-phenylhex-5-enamido)butanoic acid (**5b**).

The titled compound was separated as buff crystals, (145 mg, 68%); mp 129–131 °C; ¹H NMR (300 MHz, CDCl₃): δ 7.63–7.59 (d,

J = 16 Hz, 1H, Ph-CH=CH), δ 7.57–7.54 (m, 3H, Ar), δ 7.41–7.39 (m, 2H, Ar), δ 6.79–6.74 (d, *J* = 16 Hz, 1H, Ph-CH=CH), δ 6.48–6.45 (d, 1H, NH), δ 4.56–4.51 (m, 1H, NH-CH-CO₂H), δ 3.10–3.06 (t, 2H, CO-CH₂-CH₂-CO), δ 2.68–2.64 (t, 2H, CO-CH₂-CH₂-CO), δ 2.25–2.24 (q, 1H, NHCH-CH), δ 1.00–0.97 (m, 6H, CH-(CH₃)₂); FT-IR (*v*'_{max}, cm⁻¹): 3400–2800 (OH carboxylic), 1720, 1705 (2 C=O) 1655 (C=O amide); MS (Mwt.: 303.35): *m/z* 303.10 (M⁺, 6.57%), 186.80 (53.78%), 102.60 (55.87%), 54.30 (51.89%). Anal. Calcd for C₁₇H₂₁NO₄: C, 67.31; H, 6.98; N, 4.62. Found: C, 67.48; H, 7.15; N, 4.38.

5.1.4.4 (S,E)-2-(6-(Benzo[d][1,3]dioxol-5-yl)-4-oxohex-5-enamido)propanoic acid (**5c**).

The above compound was separated as buff crystals, (160 mg, 72%); mp 143–145 °C; ¹H NMR (300 MHz, CDCl₃): δ 7.56–7.50 (d, *J* = 16 Hz, 1H, Ph-CH=CH), δ 7.06 (s, 1H, Ph), 7.06–7.03 (d, *J* = 8 Hz, 1H, Ph), δ 6.84–6.82 (d, *J* = 8 Hz, 1H, Ph), δ 6.62–6.57 (d, *J* = 16 Hz, 1H, Ph-CH=CH), δ 6.42 (d, 1H, NH), δ 6.02 (s, 2H, OCH₂O), δ 4.55 (t, 1H, NH-CH-CO₂Me), δ 3.06–3.02 (t, 2H, CO-CH₂-CH₂-CO), δ 2.64–2.60 (t, 2H, CO-CH₂-CH₂-CO), δ 1.48–1.46 (d, 3H, NHCH-CH₃); FT-IR (*v*'_{max}, cm⁻¹): 3400–3100 (OH carboxylic), 1705, 1695 (2 C=O) 1672 (C=O amide); MS (Mwt.: 319.31): *m/z* 319 (M⁺, 7.46%), 256.80 (100%), 134.75 (73.44%). Anal. Calcd for C₁₆H₁₇NO₆: C, 60.18; H, 5.37; N, 4.39. Found: C, 60.44; H, 5.18; N, 4.42.

5.1.4.5 (S,E)-2-(6-(Benzo[d][1,3]dioxol-5-yl)-4-oxohex-5-enamido)-3-methylbutanoic acid (**5d**).

The titled compound was separated as orange oil, (165 mg, 68%); ¹H NMR (300 MHz, CDCl₃): δ 7.56–7.50 (d, *J* = 16 Hz, 1H, Ph-CH=CH), δ 7.05 (s, 1H, Ph), 7.05–7.02 (d, *J* = 8 Hz, 2H, Ph), δ 6.83–6.81 (d, *J* = 8 Hz, 1H, Ph), δ 6.62–6.57 (d, *J* = 16 Hz, 1H, Ph-CH=CH), δ 6.55 (d, 1H, NH), δ 6.01 (s, 2H, OCH₂O), δ 4.56–4.51 (m, 1H, NH-CH-CO₂Me), δ 3.06–3.02 (m, 2H, CO-CH₂-CH₂-CO), δ 2.65–2.63 (t, 2H, CO-CH₂-CH₂-CO), 2.24–2.22 (q, 1H, NHCH-CH), δ 0.99–0.95 (m, 6H, CH-(CH₃)₂); FT-IR (*v*'_{max}, cm⁻¹): 3400–2900 (OH carboxylic), 1710, 1701 (2 C=O) 1672 (C=O amide); MS (Mwt.: 347.36): *m/z* 347.35 (M⁺, 18.40%), 174.30 (82.24%). Anal. Calcd for C₁₈H₂₁NO₆: C, 62.24; H, 6.09; N, 4.03. Found: C, 62.45; H, 5.88; N, 4.15.

5.1.4.6 (S,E)-Ethyl 3-(tert-butylloxycarbonylamino)-4-phenylbut-1-ene-1-sulfonate (**7**).

To a stirred solution of ethyl (diethoxyphosphoryl)methanesulfonate (1.56 g, 6 mmol) in anhydrous THF (25 mL) at –78 °C, *n*-BuLi (2.5 M in hexane) (3.12 mL, 7.8 mmol) was added. The solution was stirred for 30 min, before a solution of **6** (1.5 g) in anhydrous THF (4 mL) was added, and the mixture was stirred at –78 °C for 1 h. The reaction was then quenched by pH 7 phosphate buffer (5 mL). The aqueous phase was extracted with ether (3 × 20 mL), the combined organic phase was washed with brine (2 × 15 mL), dried over anhydrous MgSO₄ and filtered. The filtrate was concentrated in vacuo to afford a crude yellow oil, which was purified by flash column chromatography (cyclohexane/EtOAc 3:1) (TLC stained with KMnO₄) to afford **7** as yellow crystals, (1.53 g, 72%); mp 64–65 °C; ¹H NMR (400 MHz, CDCl₃): δ 7.34–7.28 (m, 3H, Ar), δ 7.17–7.15 (d, *J* = 7 Hz, 2H, Ar), δ 6.86–6.81 (dd, *J* = 5 and 15 Hz, 1H, CH=CH-SO₃), δ 6.23–6.19 (dd, *J* = 1 and 15 Hz, 1H, CH=CH-SO₃), δ 4.65 (br s, 1H, CH-NH), δ 4.55 (br s, 1H, NH), δ 4.09–4.03 (m, 2H, SO₃-CH₂), δ 2.94–2.91 (d, 2H, CH₂-Ph), δ 1.41 (s, 9H, *t*-Bu), δ 1.34–1.3 (t, *J* = 7 Hz, 3H, SO₃-CH₂-CH₃); ¹³C NMR (100 MHz, CDCl₃): δ 154.73 (C=O), δ 147.81 (CH=CH-SO₃), δ 135.52, 129.3, 128.85, 127.28 (Ar), δ 125.05 (CH=CH-SO₃), δ 66.99 (SO₃-CH₂), δ 51.97 (CH-NH), δ 40.3 (CH₂-Ph), δ 28.23 ((CH₃)₃), δ 26.91 (C-(CH₃)₃), δ 14.77 (SO₃-CH₂-CH₃); FT-IR (*v*'_{max}, cm⁻¹): 3365 (NH), 3062 (CH=CH), 2980, 2932 (CH ali-

phatic), 1690 (C=O carbamate), 1354, 1165 (SO₂); HRMS (ESI⁺): (Mwt. 355); *m/z* found 378.1031 [M+Na]⁺, C₁₇H₂₅NO₅Na requires 378.1351.

5.1.5. (S,E)-Ethyl 3-amino-4-phenylbut-1-ene-1-sulfonate (9)

A solution of **7** (100 mg, 0.28 mmol) in 30% TFA/CH₂Cl₂ (10 mL) was stirred at rt for 1 h after which TLC (2% MeOH/EtOAc) (stained with KMnO₄) showed no starting material. The mixture was concentrated to dryness to afford the crude amine which was purified by column chromatography (gradient elution starting from EtOAc then 1% MeOH/EtOAc and increasing polarity to 5% MeOH/EtOAc) to give **9** as yellow oil, (70 mg, 98%); ¹H NMR (270 MHz, CDCl₃): δ 9.8 and 7.83 (2br s, 2H, NH₂), δ 7.33–7.30 (m, 3H, Ar), δ 7.16–7.14 (d, 2H, Ar), δ 6.88–6.8 (dd, 1H, CH=CH-SO₂), δ 6.4–6.34 (d, 1H, CH=CH-SO₂), δ 4.29 (br s, 1H, CH-NH₂), δ 4.00–3.83 (m, 2H, SO₃-CH₂), δ 3.21–3.00 (dt, 2H, CH₂-Ph), δ 1.27–1.21 (t, 3H, SO₃-CH₂-CH₃).

5.1.6. (S,E)-Ethyl 3-((E)-4-oxo-6-phenylhex-5-enamido)-4-phenylbut-1-ene-1-sulfonate (10)

To an ice-cooled solution of **3a** (56 mg, 0.27 mmol) and triethylamine (70 mg, 0.675 mmol) in methylene chloride (5 mL) stirred at –10 °C in an ice-salt bath, ethyl chloroformate (30 μL, 0.27 mmol) was added dropwise, while stirring for 10 min, after which a solution of the amine (**9**) (70 mg, 0.27 mmol) in CH₂Cl₂ (2 mL) was added dropwise. The cooling bath was then removed and the reaction was stirred at rt for 2 days until the disappearance of the starting materials as judged by TLC (EtOAc/CH₂Cl₂ 1:1) (stained with KMnO₄). The solvent was evaporated in vacuo; the residue was dissolved in EtOAc (10 mL). The organic layer was washed with 10% HCl (2 × 5 mL), then saturated Na₂CO₃ solution (2 × 5 mL), dried over anhydrous MgSO₄ and filtered. The filtrate was evaporated in vacuo to afford the crude product which was purified by column chromatography (gradient elution starting from CH₂Cl₂ then 1% EtOAc/CH₂Cl₂ and increasing polarity till 8% EtOAc/CH₂Cl₂) to finally give the titled product (**10**) as orange yellow crystals (52 mg, 44%); mp 142–143; ¹H NMR (300 MHz, CDCl₃): δ 7.61–7.57 (d, *J* = 16 Hz, 1H, Ph-CH=CH), δ 7.56–7.54 (m, 3H, Ar), δ 7.44–7.39 (m, 2H, Ar), δ 7.34–7.30 (m, 3H, Ar), δ 7.25–7.18 (d, 2H, Ar), δ 6.90–6.83 (dd, *J* = 5 and 15 Hz, 1H, CH=CH-SO₃), δ 6.76–6.70 (d, *J* = 16 Hz, 1H, Ph-CH=CH), δ 6.37–6.31 (d, *J* = 15 Hz, 1H, CH=CH-SO₃), δ 6.06–6.04 (m, 1H, NH), δ 5.01–4.99 (m, 1H, NH-CH-CH=CH), δ 4.09–4.05 (q, 2H, SO₃-CH₂), δ 3.41–3.39 (m, 2H, CH₂-Ph), δ 2.99–2.96 (m, 2H, CO-CH₂-CH₂-CO), δ 2.54–2.50 (m, 2H, CO-CH₂-CH₂-CO), δ 1.34–1.27 (m, 3H, SO₃-CH₂-CH₃); FT-IR (*ν*_{max}, cm⁻¹): 3362 (NH), 3062 (CH=CH), 3022 (CH aromatic), 2977 (CH aliphatic), 1702 (C=O ketone), 1665 (C=O amide), 1365, 1175 (SO₂); MS (Mwt.: 441.54); *m/z* 441.80 (M⁺, 1.11%), 91 (100%). Anal. Calcd for C₂₄H₂₇NO₅S: C, 65.28; H, 6.16; N, 3.17. Found: C, 65.17; H, 6.07; N, 3.32.

5.1.7. (S)-2-Acetamido-3-phenylpropan-1-ol (11)

To a solution of L-phenylalaninol (1 g, 6.6 mmol) in pyridine (20 mL) at –20 °C, acetic anhydride (0.7 mL, 7.26 mmol) was added dropwise, and the solution was stirred at –20 °C for 2 h after which TLC (EtOAc/CH₂Cl₂/MeOH 6:2:2) (stained with ninhydrin) showed no starting material. The reaction was quenched with methanol (3 mL) then evaporated in vacuo. The residue was dissolved in EtOAc (15 mL), washed with water (2 × 15 mL), brine (2 × 15 mL), dried over anhydrous MgSO₄ and filtered. The filtrate was evaporated to dryness to afford **11** as white needles which was recrystallized from EtOAc, (1.1 g, 78%); mp 98–99 °C; ¹H NMR (270 MHz, CDCl₃): δ 7.25–7.21 (m, 5H, Ar), δ 5.7 (br s, 1H, NH), δ 4.15–4.12 (m, 1H, CH-NH), δ 3.66–3.58 (m, 2H, CH₂-OH), δ 2.87–2.84 (d, 2H, CH₂-Ph), δ 2.64–2.62 (t, 1H, OH), δ 2.03 (s, 3H, Ac); HRMS (ESI⁺): (Mwt. 193); *m/z* found: 194.1168 [M+H]⁺,

C₁₁H₁₆NO₂ requires 194.1181 and 216.0987 [M+Na]⁺, C₁₁H₁₅NO₂-Na requires 216.1000.

5.1.8. (S)-2-Acetamido-3-phenylpropan-1-ol (12)

A mixture of **11** (0.193 g, 1 mmol), PDC (0.752 g, 1 mmol), activated molecular sieves (3 Å) (1 g) in anhydrous methylene chloride (5 mL) was stirred at rt for 1.5 h, after which TLC (EtOAc/CH₂Cl₂/MeOH 6:3:1) (stained with ninhydrin) showed no starting material. The mixture was diluted with ether (15 mL), filtered twice over celite, concentrated in vacuo to afford a crude yellowish oil of **12**, (0.11 g, 58%), which was used in the next step without further purification.

5.1.9. (S,E)-Ethyl 3-acetamido-4-phenylbut-1-ene-1-sulfonate (13)

To a stirred solution of ethyl (diethoxyphosphoryl)methanesulfonate (0.15 g, 0.58 mmol) in anhydrous THF (3 mL) at –78 °C, *n*-BuLi (2.5 M in hexane) (0.3 mL, 0.75 mmol) was added, the solution was stirred for 30 min, before a solution of **12** (0.11 g) in anhydrous THF (2 mL) was added, and the mixture was stirred at –78 °C for 1 h. The reaction was then quenched by pH 7 phosphate buffer (2 mL), the aqueous phase was extracted with ether (3 × 5 mL). The combined organic phase was washed with brine (2 × 10 mL), dried over MgSO₄ and filtered. The filtrate was evaporated in vacuo to afford the crude product which was purified by flash column chromatography (CH₂Cl₂/EtOAc 6:4) (TLC stained with KMnO₄) to afford **13** as pale yellow crystals, (120 mg, 70%); mp 82–83 °C; ¹H NMR (270 MHz, CDCl₃): δ 7.29–7.28 (m, 3H, Ar), δ 7.16 (d, 2H, Ar), δ 6.81–6.79 (dd, 1H, CH=CH-SO₃), δ 6.2 (dd, 1H, CH=CH-SO₃), δ 5.65 (br s, 1H, NH), δ 5.28–4.97 (m, 1H, CH-NH), δ 4.06–4.01 (q, 2H, SO₃-CH₂), δ 2.94–2.89 (d, 2H, CH₂-Ph), δ 2.03 (s, 3H, Ac), δ 1.33–1.31 (t, 3H, SO₃-CH₂-CH₃); **b** (*ν*_{max}, cm⁻¹): 3295 (NH), 3085 (CH=CH), 2973, 2895 (CH aliphatic), 1672 (C=O amide), 1352, 1170 (SO₂); HRMS (ESI⁺): (Mwt. 297); *m/z* found: 298.1111 [M+H]⁺, C₁₄H₂₀NO₄S requires 298.1113 and 320.0938 [M+Na]⁺, C₁₄H₁₉NO₄Na requires 320.0932.

5.1.10. Tetrabutylammonium (S,E)-3-acetamido-4-phenylbut-1-ene-1-sulfonate (14)

A solution of **13** (60 mg, 0.2 mmol) in anhydrous acetone (10 mL) was treated with tetrabutylammonium iodide (75 mg, 0.2 mmol) and the mixture was refluxed for 2 days till the disappearance of starting material as judged by TLC (EtOAc/CH₂Cl₂/MeOH 6:3:1) (stained with KMnO₄). The solvent was evaporated in vacuo, and the crude product was purified by flash column chromatography (EtOAc/CH₂Cl₂/MeOH 6:2:2) to afford **14** as yellow crystals, (90 mg, 88%); mp 157–158 °C; ¹H NMR (270 MHz, CD₃OD): δ 7.24–7.2 (m, 5H, Ar), δ 6.46–6.44 (dd, 1H, CH=CH-SO₃), δ 6.38 (d, 1H, CH=CH-SO₃), δ 4.22–4.17 (m, 1H, CH-NH), δ 3.3–3.29 (m, 8H, N-(CH₂)₄), δ 2.92–2.77 (dt, 2H, CH₂-Ph), 1.87 (s, 3H, Ac), δ 1.7–1.6 (m, 8H, bu₄), δ 1.5–1.2 (m, 8H, bu₄), δ 1.05–0.99 (m, 12H, bu₄); FT-IR (*ν*_{max}, cm⁻¹): 3269 (NH), 3168 (CH=CH), 2963, 2873 (CH aliphatic), 1672 (C=O amide), 1363, 1180 (SO₂); HRMS (ESI⁻): (Mwt. 510); *m/z* found: 268.0630 [M-NBu₄]⁻, C₁₂H₁₄NO₄S requires 268.0644.

5.1.11. (2R,3R)-2-Acetamido-3-(tert-butyl dimethylsilyloxy)butan-1-ol (17)

To a stirred solution of **16** (2.3 g, 7.96 mmol) in a 1:1 mixture of THF and MeOH (30 mL) at 0 °C, LiBH₄ (0.7 g, 31.82 mmol) was added portionwise, the solution was stirred at rt for 2 days, during which additional LiBH₄ (0.35 g, 15.92 mmol) in methanol (10 mL) was added. Upon disappearance of starting material as judged by TLC (EtOAc/CH₂Cl₂/MeOH 5:4.5:0.5) (stained with H₂SO₄), the reaction was quenched by addition of glacial acetic acid (7 mL) with continued stirring for 30 min. The solvent was evaporated

in vacuo. The residue was dissolved in CH_2Cl_2 (20 mL), washed with saturated NaHCO_3 (2×15 mL), brine (2×15 mL), dried over anhydrous MgSO_4 and filtered. The filtrate was evaporated to dryness to afford the crude product which was purified by flash column chromatography ($\text{EtOAc}/\text{CH}_2\text{Cl}_2/\text{MeOH}$ 5:4.5:0.5) to afford **17** as white needles, (1.75 g, 84%); mp 72–73 °C; ^1H NMR (400 MHz, CDCl_3): δ 5.95 (br s, 1H, NH), δ 4.13–4.08 (dq, $J=2$ and 6 Hz, 1H, CH–O), δ 3.87–3.81 (dt, $J=2$ and 6 Hz, 1H, CH–NH), δ 3.67–3.54 (dt, $J=6$ and 9 Hz, 2H, CH_2 –OH), δ 2.99 (br s, 1H, OH), δ 2.03 (s, 3H, Ac), δ 1.16–1.14 (d, $J=6$ Hz, 3H, CH_3 –CH–O), δ 0.89 (s, 9H, *t*-Bu), δ 0.08 (2s, 6H, 2 CH_3); ^{13}C NMR (100 MHz, CDCl_3): δ 171.25 (C=O), δ 67.28 (CH–O), δ 64.11 (CH_2 –OH), δ 56.53 (CH–NH), δ 25.78 ((CH_3)₃), δ 23.37 (Ac), δ 21.14 (CH_3), δ 17.92 (C(CH_3)₃), δ –4.27 and –5.04 (2 CH_3); FT-IR (γ_{max} , cm^{-1}): 3367 (NH), 3421 (OH), 2954, 2928, 2858 (CH aliphatic), 1677 (C=O amide); HRMS (ESI+): (Mwt. 261); m/z found: 262.1828 [$\text{M}+\text{H}$]⁺, $\text{C}_{12}\text{H}_{28}\text{NO}_3\text{Si}$ requires 262.1838, 284.1649 [$\text{M}+\text{Na}$]⁺, $\text{C}_{12}\text{H}_{27}\text{NO}_3\text{SiNa}$ requires 284.1658.

5.1.12. (2S,3R)-2-Acetamido-3-(*tert*-butyldimethylsilyloxy)butan-1-ol (**18**)

To a stirred solution of oxalyl chloride (0.19 mL, 2.25 mmol) in anhydrous methylene chloride (4 mL) at –63 °C, anhydrous DMSO (0.213 mL, 3 mmol) in CH_2Cl_2 (4 mL) was added over 10 min. Immediately following, a solution of **17** (0.392 g, 1.5 mmol) in CH_2Cl_2 (6 mL) was added over 10 min, the reaction was stirred at –63 °C for 30 min. Triethylamine (0.84 mL, 6 mmol) was then added over 5 min, and the mixture was stirred at –63 °C for an additional 30 min. The reaction was then allowed to warm to rt, 20% aqueous KHSO_3 (5 mL) was added, then cyclohexane (10 mL), and the reaction was stirred vigorously at rt till the separation of 2 phases. The layers were separated, the aqueous phase was extracted with CH_2Cl_2 (3×10 mL), the combined organic phase was washed with saturated NaHCO_3 solution (2×10 mL), brine (2×10 mL), dried over anhydrous MgSO_4 and filtered. The filtrate was evaporated to dryness to afford the crude aldehyde (**18**) as yellowish oil (0.39 g, 100%), which was used in the next step without further purification. ^1H NMR (270 MHz, CDCl_3): δ 9.59 (s, 1H, CH=O), δ 6.25 (br s, 1H, NH), δ 4.54–4.49 (m, 2H, CH=NH and CH=O), δ 2.11 (s, 3H, Ac), δ 1.17 (d, 3H, CH_3 –CH–O), δ 0.89 (s, 9H, *t*-Bu), δ 0.08–0.06 (2s, 6H, 2 CH_3).

5.1.13. (3R,4R,E)-Ethyl 3-acetamido-4-(*tert*-butyldimethylsilyloxy)pent-1-ene-1-sulfonate (**19**)

To a stirred solution of ethyl (diethoxyphosphoryl)methanesulfonate (0.38 g, 1.46 mmol) in anhydrous THF (6 mL) at –78 °C, *n*-BuLi (2.5 M in hexane) (0.88 mL, 2.19 mmol) was added. The solution was stirred for 30 min, after which a solution of **18** (0.39 g) in anhydrous THF (4 mL) was added, and the reaction was stirred at –78 °C for 1 h. The reaction was then quenched by pH 7 phosphate buffer (5 mL), allowed to warm to rt, then concentrated in vacuo. The residue was dissolved in CH_2Cl_2 (15 mL), washed with brine (2×10 mL), dried over MgSO_4 and filtered. The filtrate was evaporated in vacuo to afford the crude product which was purified by flash chromatography ($\text{EtOAc}/\text{CH}_2\text{Cl}_2/\text{cyclohexane}$ 3:4:2) (TLC stained with KMnO_4) to afford **19** as white needles, (0.314 g, 59%); mp 86–87 °C; ^1H NMR (400 MHz, CDCl_3): δ 6.85–6.8 (dd, $J=5$ and 15 Hz, 1H, CH=CH– SO_3), δ 6.31–6.27 (dd, $J=2$ and 15 Hz, 1H, CH=CH– SO_3), δ 5.91–5.89 (d, 1H, NH), δ 4.59–4.57 (m, 1H, CH–NH), δ 4.18–4.10 (q, $J=7$ Hz, 2H, SO_3 – CH_2), δ 4.08–4.03 (dq, $J=2$ and 6 Hz, 1H, CH–O), δ 2.08 (s, 3H, Ac), δ 1.38–1.34 (t, $J=7$ Hz, 3H, SO_3 – CH_2 – CH_3), δ 1.19–1.18 (d, $J=6$ Hz, 3H, CH_3 –CH–O), δ 0.88 (s, 9H, *t*-Bu), δ 0.07 (2s, 6H, 2 CH_3); ^{13}C NMR (100 MHz, CDCl_3): δ 169.98 (C=O), δ 147.05 (CH=CH– SO_3), δ 125.76 (CH=CH– SO_3), δ 69.1 (CH–OH), δ 66.9 (SO_3 – CH_2), δ 55.13 (CH–NH), δ 25.74 ((CH_3)₃), δ 23.21 (Ac), δ 20.98 (CH_3),

δ 17.92 (C(CH_3)₃), δ 14.83 (SO_3 – CH_2 – CH_3), δ –4.48 and –4.9 (2 CH_3); FT-IR (γ_{max} , cm^{-1}): 3354 (NH), 3062 (CH=CH), 2963, 2943, 2865 (CH aliphatic), 1667 (C=O amide), 1355, 1175 (SO_2); HRMS (ESI+): (Mwt. 365); m/z found: 366.1782 [$\text{M}+\text{H}$]⁺, $\text{C}_{15}\text{H}_{32}\text{NO}_5\text{Si}$ requires 366.1770 and 388.1595 [$\text{M}+\text{Na}$]⁺, $\text{C}_{15}\text{H}_{31}\text{NO}_5\text{SiNa}$ requires 388.1590.

5.1.14. (3R,4R,E)-Ethyl 3-acetamido-4-hydroxypent-1-ene-1-sulfonate (**20**)

To a solution of **19** (0.25 g, 0.685 mmol) in THF (10 mL), 70% HF/pyridine (0.7 mL) was added, and the resulting mixture was stirred at rt for 3 h after which TLC (2% MeOH/EtOAc) (stained with KMnO_4) revealed the disappearance of starting material. The reaction was quenched by addition of saturated NaHCO_3 solution (5 mL). The mixture was concentrated in vacuo, the residue was dissolved in EtOAc (10 mL), washed with saturated NaHCO_3 (3×15 mL), H_2O (2×10 mL), brine (2×15 mL), dried over anhydrous MgSO_4 and filtered. The filtrate was evaporated to dryness to afford the crude product which was purified by flash column chromatography (1% MeOH/EtOAc) to give **20** as white needles, (148 mg, 86%); mp 112–114 °C; ^1H NMR (270 MHz, CD_3OD): 6.95–6.88 (dd, 1H, CH=CH– SO_3), δ 6.51–6.44 (d, 1H, CH=CH– SO_3), δ 4.62–4.61 (br s, 1H, CH–NH), δ 4.20–4.12 (q, 2H, SO_3 – CH_2), δ 3.96–3.94 (m, 1H, CH–OH), δ 2.04–1.99 (s, 3H, Ac), δ 1.36–1.31 (t, 3H, SO_3 – CH_2 – CH_3), δ 1.17–1.09 (d, 3H, CH_3 –CH–O); FT-IR (γ_{max} , cm^{-1}): 3475 (OH), 3285 (NH), 3115 (CH=CH), 2958, 2885 (CH aliphatic), 1672 (C=O amide), 1365, 1172 (SO_2); HRMS (ESI+): (Mwt. 251); m/z found: 252.0906 [$\text{M}+\text{H}$]⁺, $\text{C}_9\text{H}_{18}\text{NO}_5\text{S}$ requires 252.0906 and 274.0721 [$\text{M}+\text{Na}$]⁺, $\text{C}_9\text{H}_{17}\text{NO}_5\text{SNa}$ requires 274.0725.

5.2. Biological evaluation

5.2.1. Materials and methods

5.2.1.1 Cell culture and culture media.

Human hepatoma cells (Huh7.5) were maintained in Dulbecco's modified eagle's medium (DMEM) (Gibco) supplemented with 1% *L*-glutamine (Gibco), 1% penicillin, 1% streptomycin (Gibco), 1× nonessential amino acids (Gibco) and 10% fetal bovine serum (FBS) (Omega Scientific). Cell lines were passaged twice weekly after treatment with 0.05% trypsin–0.02% EDTA and seeding at a dilution of 1:5. Subconfluent Huh7.5 cells were trypsinized and collected by centrifugation at 700g for 5 min. The cells were then washed three times in ice-cold RNase-free phosphate-buffered saline (PBS) (BioWhittaker) and resuspended at 1.5×10^7 cells/mL in PBS.

5.2.1.2 Transfection and drug treatment.

The plasmid FL-J6/JFH-5'C19Rluc2Aubi that consists of the full-length HCV genome (genotype 2a) and expresses *Renilla* luciferase (Rluc) was transfected into Huh7.5 cells using Lipofectamine 2000 (Invitrogen) following manufacturer's specifications. After 24 h, cells were pooled and seeded in 96-well plates ($2\text{--}3 \times 10^4$ cells/well). Cells were grown in quadruplicates in the presence of serial dilutions of the test compounds (**4a–f**, **5b,c**, **7**, **8**, **10**, **13**, **1420**) dissolved in DMSO. DMSO was used as a negative control, while the NS3 protease inhibitor boceprevir (SCH503034) was used as positive control. After 48 h, cells were subjected to luciferase assays and alamarBlue-based viability assays.

5.2.1.3 Assay protocols.

(i) Luciferase assay: Viral RNA replication was determined using *Renilla* luciferase assays (Promega). Cells were washed with PBS and shaken in lysis buffer according to the manufacturer's protocol. After 15 min incubation at –80 °C and thawing, luciferase assay buffer containing the assay substrate was injected, and luciferase

activity was measured using a Berthold LB96V luminometer. Signal was normalized relative to samples grown in the presence of DMSO as a negative control. Experiments were repeated 3 times, each time with 4 replicates.

(ii) *Viability assay*: Cells were incubated for 2 h at 37 °C in the presence of either 10% alamarBlue reagent (Invitrogen) or for 1 h in the presence of 10% Prestoblue reagent (Invitrogen) to assess cytotoxicity. Fluorescence was detected using FLEXstationII 384 (Molecular Devices). Signal was normalized as described above.

5.2.1.4 Statistical analysis.

EC₅₀ and CC₅₀ values were measured by fitting data to a 3-parameter logistic curve using the formula:

$$Y = a + (b - a) / (1 + 10^{(X-c)})$$

where *a*, *b*, and *c* represent minimum binding, maximum binding, and log EC₅₀ or log CC₅₀, respectively (BioDataFit; Chang Bioscience).

5.3. Molecular modeling

5.3.1. Preparing ligand structures

All the studied compounds were using Maestro Interface (version 9.2, Schrödinger, LLC, NY, 2011) and geometries were optimized with using OPLS_2005, the implementation of the OPLS-AA forcefield⁵⁵ in MacroModel (version 9.9, Schrödinger, LLC, NY, 2011), combined with GB/SA implicit solvent model.⁵⁶ Carboxylate esters and vinyl sulfonate esters were modeled as the neutral species while vinyl sulfonate tetrabutylammonium salts were modeled as the negatively charged de-protonated species. Compounds **5b** and **5c** were modeled as the ionized carboxylate form as predicted by Epik.⁵⁷

5.3.2. Preparing enzyme structures

Complexes of HCV NS3/4A protease with various ligands were downloaded from the Protein Data Bank. For each crystal structure, hydrogens were added, water molecules were removed and bond orders for proteins and ligand were corrected using Maestro Protein Preparation Wizard. Partial charges were calculated from OPLS-AA⁵⁵ forcefield while protonation states and oxidation states for metals were assigned by Epik.⁵⁷ Orientations of added hydrogens were extensively sampled for optimal H-bond formation and the model was then refined by minimization to heavy-atom RMSD of 0.3 Å to the crystal structure geometry. Eventually, an all-atom ligand–protein complex with properly assigned ionization states and atomic charges was available that could be used in subsequent modeling steps.

5.3.3. Docking of the non-covalent binders

Non-covalent docking study was performed for all the studied compounds using Glide software (version 5.7, Schrödinger, LLC, NY, 2011). The crystal structure of HCV protease with danoprevir (ITMN191) was used to generate the docking grid (PDB: 3M5L, resolution 1.25 Å).⁴⁸ Terminal hydroxyl groups of Tyr56, Thr60 and Ser89 were treated as 'rotatable groups' within the created grid. Number of poses allowed to pass through the initial Glide screens was increased to 100,000. The energy window for keeping initial poses was set to 100.0 kcal/mol and the best 1000 poses for each ligand were kept for energy minimization. Atoms with partial charges <0.15 were scaled down in size by a factor of 0.8 to soften the potential for non-polar parts of the ligand. The output for each ligand included a maximum of 5 distinct poses. All resultant poses were visually inspected and poses where the oxyanion hole was not occupied were excluded. Glide calculates per-residue interaction energies as the sum of OPLS_2005 non-bonded terms (van

der Waals, Columbic and H-bond terms) for all residues within 12.0 Å distance from any found pose. Interactions fingerprints were calculated for studied compounds by summing per-residue interaction energies for amino acids comprising HCV protease oxyanion hole (Gly137 + Ala139) and the three sub-pockets S1 (Ala157 + Ile132 + Phe154), S2 (Ala157 + Arg155 + His57) and S3 (Ile132 + Ala157 + Ser159 + Lys136 + Arg161). Interaction fingerprints for studied compounds are given in Table 3.

Due to its relatively larger size and higher flexibility, compound (**10**) was docked using a specialized induced-fit docking protocol⁵⁸ through a combination of Glide (version 5.7, Schrödinger, LLC, NY, 2011) and Prime (version 3.0, Schrödinger, LLC, NY, 2011). After the initial Glide docking, amino acids within 5.0 Å radius around any suggested pose were considered as flexible, and their side chain conformations were optimized by Prime. Up to 50 poses were retained for each calculation within an energy window of 40.0 kcal/mol. Poses were finally energy minimized, re-scored and prioritized by Glide SP scoring.

5.3.4. Covalent Docking for (10)

Docking of vinyl sulfonate (**10**) was performed using the covalent docking facility in Prime. Crystal structure of (**1**) covalently bound to catalytic Ser139 of HCV NS3/4A protease was used (PDB: 1W3C).²² Downloaded crystal structure was processed into a full-atom optimized model as described previously. Ligand structure was deleted, Ser139 hydroxyl hydrogen was added, Val132 was mutated into Ile and the protein alone was energy minimized again to a gradient of 0.05 kJ/mol Å. The Ser139 terminal O–H bond was specified as the 'receptor bond to break'. Vinyl sulfonate double bonds were reduced to single bonds to match the proposed ligand structure upon binding; then modified structures were re-minimized. The ligand reactive group was set up to match the pattern H₂C–C–S; such that any of the two hydrogens furthest from sulfur could be the leaving atom. Finally, protein residues within 8.0 Å from Ser139 were included in Prime conformational sampling and optimization.

Supplementary data

Supplementary data associated with this article can be found, in the online version, at <http://dx.doi.org/10.1016/j.bmc.2013.03.017>.

References and notes

- Naggie, S.; Patel, K.; McHutchison, J. *J. Antimicrob. Chemother.* **2010**, *65*, 2063.
- Njoroge, F. G.; Chen, K. X.; Shih, N.-Y.; Piwinski, J. *J. Acc. Chem. Res.* **2008**, *41*, 50.
- Chatel-Chaix, L.; Baril, M.; Lamarre, D. *Viruses* **2010**, *2*, 1752.
- Li, X.; Zhang, Y.-K.; Liu, Y.; Ding, C. Z.; Zhou, Y.; Li, Q.; Plattner, J. J.; Baker, S. J.; Zhang, S.; Kazmierski, W. M.; Wright, L. L.; Smith, G. K.; Grimes, R. M.; Crosby, R. M.; Creech, K. L.; Carballo, L. H.; Slater, M. J.; Jarvest, R. L.; Thommes, P.; Hubbard, J. A.; Convery, M. A.; Nassau, P. M.; McDowell, W.; Skarzynski, T. J.; Qian, X.; Fan, D.; Liao, L.; Ni, Z.-J.; Pennicott, L. E.; Zou, W.; Wright, J. *Bioorg. Med. Chem. Lett.* **2010**, *20*, 5695.
- Birerdinc, A.; Younossi, Z. M. *Expert Opin. Emerg. Drugs* **2010**, *15*, 535.
- Pearlman, B. L. *Lancet Infect. Dis.* **2012**, *12*, 717.
- Esteban, R.; Buti, M. *Best Pract. Res. Clin. Gastroenterol.* **2012**, *26*, 445.
- Alexopoulou, A.; Papatheodoridis, G. V. *World J. Gastroenterol.* **2012**, *18*, 6060.
- Penin, F.; Dubuisson, J.; Rey, F. A.; Moradpour, D.; Pawlatsky, J. M. *Hepatology* **2004**, *39*, 5.
- Appel, N.; Schaller, T.; Penin, F.; Bartenschlager, R. *J. Biol. Chem.* **2006**, *281*, 9833.
- Melnikova, I. *Nat. Rev. Drug Disc.* **2011**, *10*, 93.
- Lamarre, D.; Anderson, P. C.; Bailey, M.; Beaulieu, P.; Bolger, G.; Bonneau, P.; Bos, M.; Cameron, D. R.; Cartier, M.; Cordingley, M. G.; Faucher, A.-M.; Goudreau, N.; Kawai, S. H.; Kukulj, G.; Lagace, L.; LaPlante, S. R.; Narjes, H.; Poupart, M.-A.; Rancourt, J.; Sentjens, R. E.; St George, R.; Simoneau, B.; Steinmann, G.; Thibeault, D.; Tsantrizos, Y. S.; Weldon, S. M.; Yong, C.-L.; Llinas-Brunet, M. *Nature (London, U.K.)* **2003**, *426*, 186.
- Yao, N.; Reichert, P.; Taremi, S. S.; Prosser, W. W.; Weber, P. C. *Structure (London)* **1999**, *7*, 1353.
- Llinas-Brunet, M.; Bailey, M. D.; Goudreau, N.; Bhardwaj, P. K.; Bordeleau, J.; Bos, M.; Bousquet, Y.; Cordingley, M. G.; Duan, J.; Forgione, P.; Garneau, M.;

- Ghiro, E.; Gorys, V.; Goulet, S.; Halmos, T.; Kawai, S. H.; Naud, J.; Poupart, M.-A.; White, P. W. *J. Med. Chem.* **2010**, *53*, 6466.
15. LaPlante, S. R.; Llinas-Brunet, M. *Curr. Med. Chem.: Anti-Infect. Agents* **2005**, *4*, 111.
16. Bennett, F.; Huang, Y.; Hendrata, S.; Lovey, R.; Bogen, S. L.; Pan, W.; Guo, Z.; Prongay, A.; Chen, K. X.; Arasappan, A.; Venkatraman, S.; Velazquez, F.; Nair, L.; Sannigrahi, M.; Tong, X.; Pichardo, J.; Cheng, K.-C.; Girijavallabhan, V. M.; Saksena, A. K.; Njoroge, F. G. *Bioorg. Med. Chem. Lett.* **2010**, *20*, 2617.
17. Arasappan, A.; Bennett, F.; Bogen, S. L.; Venkatraman, S.; Blackman, M.; Chen, K. X.; Hendrata, S.; Huang, Y.; Huelgas, R. M.; Nair, L.; Padilla, A. I.; Pan, W.; Pike, R.; Pinto, P.; Ruan, S.; Sannigrahi, M.; Velazquez, F.; Vibulbhan, B.; Wu, W.; Yang, W.; Saksena, A. K.; Girijavallabhan, V.; Shih, N.-Y.; Kong, J.; Meng, T.; Jin, Y.; Wong, J.; McNamara, P.; Prongay, A.; Madison, V.; Piwinski, J. J.; Cheng, K.-C.; Morrison, R.; Malcolm, B.; Tong, X.; Ralston, R.; Njoroge, F. G. *ACS Med. Chem. Lett.* **2010**, *1*, 64.
18. Venkatraman, S.; Bogen, S. L.; Arasappan, A.; Bennett, F.; Chen, K.; Jao, E.; Liu, Y.-T.; Lovey, R.; Hendrata, S.; Huang, Y.; Pan, W.; Parekh, T.; Pinto, P.; Popov, V.; Pike, R.; Ruan, S.; Santhanam, B.; Vibulbhan, B.; Wu, W.; Yang, W.; Kong, J.; Liang, X.; Wong, J.; Liu, R.; Butkiewicz, N.; Chase, R.; Hart, A.; Agrawal, S.; Ingravallo, P.; Pichardo, J.; Kong, R.; Baroudy, B.; Malcolm, B.; Guo, Z.; Prongay, A.; Madison, V.; Broske, L.; Cui, X.; Cheng, K.-C.; Hsieh, T. Y.; Brisson, J.-M.; Prelusky, D.; Korfmacher, W.; White, R.; Bogdanowich-Knipp, S.; Pavlovsky, A.; Bradley, P.; Saksena, A. K.; Ganguly, A.; Piwinski, J.; Girijavallabhan, V.; Njoroge, F. G. *J. Med. Chem.* **2006**, *49*, 6074.
19. Perni, R. B.; Almqvist, S. J.; Byrn, R. A.; Chandorkar, G.; Chaturvedi, P. R.; Courtney, L. F.; Decker, C. J.; Dinehart, K.; Gates, C. A.; Harbeson, S. L.; Heiser, A.; Kalkeri, G.; Kolaczowski, E.; Lin, K.; Luong, Y.-P.; Rao, B. G.; Taylor, W. P.; Thomson, J. A.; Tung, R. D.; Wei, Y.; Kwong, A. D.; Lin, C. *Antimicrob. Agents Chemother.* **2006**, *50*, 899.
20. Colarusso, S.; Gerlach, B.; Koch, U.; Muraglia, E.; Conte, I.; Stansfield, I.; Matassa, V. G.; Narjes, F. *Bioorg. Med. Chem. Lett.* **2002**, *12*, 705.
21. Han, W.; Hu, Z.; Jiang, X.; Decicco, C. P. *Bioorg. Med. Chem. Lett.* **2000**, *10*, 711.
22. Ontoria, J. M.; Di Marco, S.; Conte, I.; Di Francesco, M. E.; Gardelli, C.; Koch, U.; Matassa, V. G.; Poma, M.; Steinkuehler, C.; Volpari, C.; Harper, S. *J. Med. Chem.* **2004**, *47*, 6443.
23. Berg, M.; Van der Veken, P.; Joossens, J.; Muthusamy, V.; Breugelmanns, M.; Moss, C. X.; Rudolf, J.; Cos, P.; Coombs, G. H.; Maes, L.; Haemers, A.; Mottram, J. C.; Augustyns, K. *Bioorg. Med. Chem. Lett.* **2001**, *2010*, 20.
24. Lee, J. T.; Chen, D. Y.; Yang, Z.; Ramos, A. D.; Hsieh, J. J. D.; Bogoy, M. *Bioorg. Med. Chem. Lett.* **2009**, *19*, 5086.
25. Ettari, R.; Nizi, E.; DiFrancesco, M. E.; Dude, M. A.; Pradel, G.; Vicík, R.; Schirmeister, T.; Micale, N.; Grasso, S.; Zappalà, M. *J. Med. Chem.* **2008**, *51*, 988.
26. Reddick, J. J.; Cheng, J.; Roush, W. R. *Org. Lett.* **1967**, *2003*, 5.
27. Roush, W. R.; Gwaltney, S. L.; Cheng, J.; Scheidt, K. A.; McKerrow, J. H.; Hansell, E. *J. Am. Chem. Soc.* **1998**, *120*, 10994.
28. Ettari, R.; Bova, F.; Zappalà, M.; Grasso, S.; Micale, N. *Med. Res. Rev.* **2010**, *30*, 136.
29. Abouzid, K. A. M.; Youssef, K. M.; Ahmed, A. A. E.; Al-Zuhair, H. H. *Med. Chem. Res.* **2005**, *14*, 26.
30. Ismail, M. A. H.; Lehmann, J.; Abou El Ella, D. A.; Albohy, A.; Abouzid, K. A. M. *Med. Chem. Res.* **2009**, *18*, 725.
31. Chen, K. X.; Njoroge, F. G.; Pichardo, J.; Prongay, A.; Butkiewicz, N.; Yao, N.; Madison, V.; Girijavallabhan, V. *J. Med. Chem.* **2005**, *48*, 6229.
32. Konradi, A. W.; Kemp, S. J.; Pedersen, S. F. *J. Am. Chem. Soc.* **1994**, *116*, 1316.
33. Carretero, J. C.; Demillequand, M.; Ghosez, L. *Tetrahedron* **1987**, *43*, 5125.
34. Gennari, C.; Longari, C.; Ressel, S.; Salom, B.; Mielgo, A. *Eur. J. Org. Chem.* **1998**, 945.
35. Enders, D.; Harnying, W. *Synthesis* **2004**, 2910.
36. Hvidt, T.; Szarek, W. A.; Maclean, D. B. *Can. J. Chem.* **1988**, *66*, 779.
37. Czernecki, S.; Georgoulis, C.; Stevens, C. L.; Vijayakumaran, K. *Tetrahedron Lett.* **1985**, *26*, 1699.
38. Herscovici, J.; Egron, M. J.; Antonakis, K. *J. Chem. Soc., Perkin Trans. 1* **1967**, 1982.
39. Torrini, I.; Zecchini, G. P.; Agrosi, F.; Paradisi, M. P. *J. Heterocycl. Chem.* **1986**, *23*, 1459.
40. Kawulka, K. E.; Sprules, T.; Diaper, C. M.; Whittall, R. M.; McKay, R. T.; Mercier, P.; Zuber, P.; Vederas, J. C. *Biochemistry* **2004**, *43*, 3385.
41. Wipf, P.; Reeves, J. T.; Balachandran, R.; Day, B. W. *J. Med. Chem.* **1901**, *2002*, 45.
42. Kanemoto, M.; Murata, M.; Oishi, T. *J. Org. Chem.* **2009**, *74*, 8810.
43. Pinot, E.; Guy, A.; Fournial, A.; Balas, L.; Rossi, J.-C.; Durand, T. *J. Org. Chem.* **2008**, *73*, 3063.
44. Blight, K. J.; McKeating, J. A.; Rice, C. M. *J. Virol.* **2002**, *76*, 13001.
45. Prongay, A. J.; Guo, Z.; Yao, N.; Pichardo, J.; Fischmann, T.; Strickland, C.; Myers, J.; Weber, P. C.; Beyer, B. M.; Ingram, R.; Hong, Z.; Prorise, W. W.; Ramanathan, L.; Taremi, S. S.; Yarosh-Tomaine, T.; Zhang, R.; Senior, M.; Yang, R.-S.; Malcolm, B.; Arasappan, A.; Bennett, F.; Bogen, S. L.; Chen, K.; Jao, E.; Liu, Y.-T.; Lovey, R. G.; Saksena, A. K.; Venkatraman, S.; Girijavallabhan, V.; Njoroge, F. G.; Madison, V. *J. Med. Chem.* **2007**, *50*, 2310.
46. Einav, S.; Sobol, Hadas D.; Gehrig, E.; Glenn, Jeffrey S. *J. Infect. Dis.* **2010**, *202*, 65.
47. Einav, S.; Gerber, D.; Bryson, P. D.; Sklan, E. H.; Elazar, M.; Maerkl, S. J.; Glenn, J. S.; Quake, S. R. *Nat. Biotechnol.* **2008**, *26*, 26.
48. Romano, K. P.; Ali, A.; Royer, W. E.; Schiffer, C. A. *Proc. Natl. Acad. Sci. U.S.A.* **2010**, *107*, 20986.
49. Thibeault, D.; Bousquet, C.; Gingras, R.; Lagace, L.; Maurice, R.; White, P. W.; Lamarre, D. *J. Virol.* **2004**, *78*, 7352.
50. Hagel, M.; Niu, D.; St. Martin, T.; Sheets, M. P.; Qiao, L.; Bernard, H.; Karp, R. M.; Zhu, Z.; Labenski, M. T.; Chaturvedi, P.; Nacht, M.; Westlin, W. F.; Petter, R. C.; Singh, J. *Nat. Chem. Biol.* **2011**, *7*, 22.
51. Cummings, M. D.; Lindberg, J.; Lin, T. I.; de Kock, H.; Lenz, O.; Lilja, E.; Felländer, S.; Baraznenok, V.; Nystrom, S.; Nilsson, M.; Vrang, L.; Edlund, M.; Rosenquist, A.; Samuelsson, B.; Raboisson, P.; Simmen, K. *Angew. Chem., Int. Ed.* **2010**, *49*, 1652.
52. Bianchi, E.; Orrù, S.; DalPiaz, F.; Ingenito, R.; Casbarra, A.; Biasiol, G.; Koch, U.; Pucci, P.; Pessi, A. *Biochemistry* **1999**, *38*, 13844.
53. Bäck, M.; Johansson, P. O.; Wängsell, F.; Thorstensson, F.; Kvarnström, I.; Ayasa, S.; Wähling, H.; Pelcman, M.; Jansson, K.; Lindström, S.; Wallberg, H.; Classon, B.; Rydergård, C.; Vrang, L.; Hamelink, E.; Hallberg, A.; Rosenquist, S.; Samuelsson, B. *Bioorg. Med. Chem.* **2007**, *15*, 7184.
54. Tsantrizos, Y. S.; Bolger, G.; Bonneau, P.; Cameron, D. R.; Goudreau, N.; Kukolj, G.; LaPlante, S. R.; Llinas-Brunet, M.; Nar, H.; Lamarre, D. *Angew. Chem., Int. Ed.* **2003**, *42*, 1356.
55. Jorgensen, W. L.; Maxwell, D. S.; Tirado-Rives, J. *J. Am. Chem. Soc.* **1996**, *118*, 11225.
56. Still, W. C.; Tempczyk, A.; Hawley, R. C.; Hendrickson, T. *J. Am. Chem. Soc.* **1990**, *112*, 6127.
57. Shelley, J. C.; Cholleti, A.; Frye, L. L.; Greenwood, J. R.; Timlin, M. R.; Uchimaya, M. *J. Comput.-Aided Mol. Des.* **2007**, *21*, 681.
58. Sherman, W.; Day, T.; Jacobson, M. P.; Friessner, R. A.; Farid, R. *J. Med. Chem.* **2006**, *49*, 534.